Functional analysis of two novel effector candidates of Arabidopsis heterotrimeric G protein β subunit, AGB1

（シロイヌナズナのヘテロ三量体 G タンパク質 β サブユニット（AGB1）の新奇エフェクター候補の機能解析）

劉　華

Contents

Chapter 1

General introduction

Eukaryotes are able to cope with the dynamic variations in the surrounding environment by activating intracellular signaling pathways. Transmembrane receptors associated with the plasma membrane are the primary elements in signaling pathways and therefore perform critical functions in organism survival.

1.1 G-protein-coupled receptors (GPCRs)

In human, G-protein-coupled receptors (GPCRs) are the largest families of membrane proteins, which were characterized by the presence of seven membrane-spanning α-helical segments separated by alternating intracellular and extracellular loop regions (Rosenbaum *et al*., 2009). Generally, agonist binding to GPCRs leads to the rearrangements of GPCRs transmembrane helix (Scheerer *et al*., 2008; Park *et al*., 2008) resulting in the activation of G proteins. Individual GPCRs have unique combinations involved in G-proteins as well as G-protein-independent signaling pathways and complex regulatory processes. GPCRs perform a variety of functions, such as the light response, odor, taste, neurotransmitters, and hormones. Their ligands are diverse, including small organic molecules, lipids, ions, hormones, polypeptides, and glycoproteins (Gether, 2000).

1.2 Heterotrimeric guanine nucleotide-binding proteins (G proteins)

An evolutionarily ancient mechanism for sensing extracellular cues involves the heterotrimeric guanine nucleotide-binding proteins (G proteins). G protein consists of

Gα, Gβ, and Gγ subunits, with Gα and Gγ subunits carrying lipid modifications that enable membrane attachment (Casey, 1995). G protein complexes link ligand perception via GPCRs in the plasma membrane. G proteins bind to the intracellular side of GPCRs. The agonist-stimulated GPCR trigger the Gα to release GDP, thus enabling the Gα to bind GTP. GTP binding is accompanied by structural rearrangements resulting in dissociation of the Gβγ dimer (Fig. 1-1). Free Gα monomer or Gβγ dimer, or both, activate the downstream effectors. Gβγ subunit signaling is terminated by hydrolysis of GTP, and Gβγ dimer signaling is terminated by reassociation with Gα subunits in a way that sequesters the protein recognition surface on these subunits. Genes that encode G protein elements have been identified in amoebae, fungi, plants, and animals. In human genome, there are 23 Gα, 5 Gβ, 12 Gγ subunits (Malbon, 2005), and more than 800 predicted GPCRs (Pierce *et al*., 2002). In addition to the plasma membrane, mammalian and other eukaryotic G proteins are associated with the cytoskeleton, nucleus and endomembranes (Willard and Crouch, 2000; Gotta and Ahringer, 2001; Simonds *et al*., 2004). G-protein-coupled signaling pathways are involved in numerous mammalian physiological processes (Hampoelz and Knoblich, 2004; Malbon, 2005). Among the multicellular eukaryotes, plants may have the simplest repertoire of G protein elements. The Arabidopsis and rice (*Oryza sativa*) genomes contain a simple G protein system with one Gα gene, one Gβ gene and three or four Gγ genes (Weiss *et al*., 1994; Mason and Botella, 2000, 2001; Kato *et al*., 2004; Chakravorty *et al*., 2012). Heterotrimeric G proteins play roles in various signal transductions, such as auxin (Ishida *et al*., 1993), abscisic acid (Fairley-Grenot and Assmann, 1991), gibberellin (Jones *et al*., 1998; Ueguchi-Tanaka *et al*., 2000), pathogens (Beffa *et al*., 1995), blue light (Warpeha *et al*., 1991), and red light (Neuhaus *et al*., 1993). Genetic evidence has indicated that abscisic acid (Wang *et al*., 2001) and brassinosteroids (Ullah *et al*., 2002) use a heterotrimeric G protein in signal transduction. It is apparent that some signaling functions are cell-type dependent, which could result from interaction with different receptors/effectors expressed in different cell types or from the balance of Gα one Gβγ subunits in plant cell, perhaps working antagonistically (Jones and

Assmann, 2004).

1.3 Effectors of heterotrimeric G proteins in Arabidopsis

The G-protein-activated enzymes were collectively called effectors. Arabidopsis has only one Gα gene (*GPA1*, Jones and Assmann 2004)), one Gβ gene (*AGB1*, Jones and Assmann 2004) and three Gγ genes (*AGG1*, *AGG2*, *AGG3*, Mason and Botella, 2000, 2001; Chakravorty *et al*., 2011). In Arabidopsis, *AGB1*-deficiency causes changes in morphology and sensitivities to various stimuli (Pandey *et al*., 2006; Trusov *et al*., 2007, 2009; Wang *et al*., 2007; Wei *et al*., 2008), suggesting that effectors regulated by Gβγ have important physiological roles. Recently, a set of Arabidopsis heterotrimeric G protein interactome genes were identified by using two-hybrid complementation in yeast, which reveals a novel role for G-proteins in regulating cell wall modification (Klopffleisch *et al*., 2011). N-MYC DOWNREGULATED-LIKE1 (NDL1) and an acireductone dioxygenase-like protein (ARD1) physically interact with AGB1 in Arabidopsis (Mudgil *et al*. 2009; Friedman *et al*., 2011). However, the molecular mechanisms underlying the AGB1-mediated signaling remain to be elucidated.

Using full-length AGB1 as bait, a Y2H screen of the Arabidopsis leaf library was performed to identify AGB1-interacting proteins. Even on high-stringency selection media, which lack histidine and adenine, more than 3600 positive clones were obtained. Yeast colony PCR with an *AGG1*-specific primer revealed that 60-70% of these clones expressed AGG1. Plasmid inserts from non-*AGG1* clones were amplified by yeast colony PCR using a vector-specific primer pair and sequenced. An Arabidopsis U-box E3 ubiquitin ligase Plant U-box 20 (PUB20) was identified as a possible interactor of AGB1 and was characterized (Kobayashi *et al.*, 2012). In this research, a conserved RNA-binding motif protein (AtRBM22) and a type-2C protein phosphatase (AtPP2C52) were identified as novel AGB1-interacting partners.

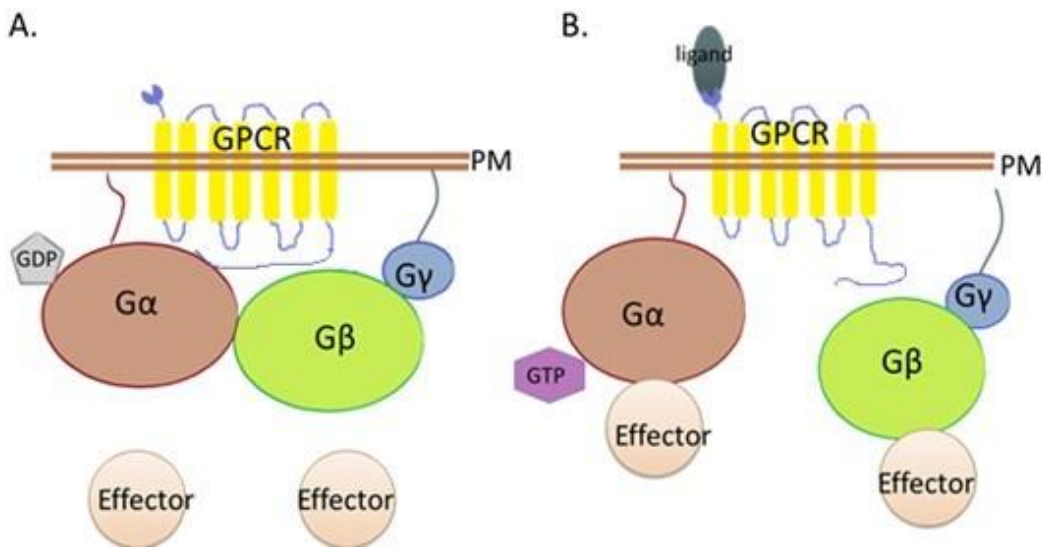

Fig. 1-1 Heterotrimeric G-protein paradigm. The heterotrimeric G protein consists of three different subunits, Gα (40-46 kDa), Gβ (37-44 kDa), and Gγ (6-9 kDa) subunits, with Gα and Gγ subunits carrying lipid modifications that enable membrane attachment. GPCR physically interacts with Gα. Gα, Gβ and Gγ form a heterotrimeric complex in the inactive state (A). Binding of an agonist (*i.e.* an activating ligand) to a specific GPCR leads to the conversion of an inactive G protein to its active conformation (B). The Gα binds to the top surface of the Gβ propeller. PM, plasma membrane.

Chapter 2

Translocation of an RNA-binding motif protein (AtRBM22) to nuclear speckles in Arabidopsis thaliana

2.1 Abstract

Nuclear speckles are subnuclear structures that may function in storage, assembly and modification of pre-mRNA splicing factors. One such factor is RNA-binding motif protein RBM22. In this study, an Arabidopsis RBM22 (AtRBM22) was identified as a novel target of the heterotrimeric G protein β subunit (AGB1). AtRBM22 was located in the nuclei and was found to interact with AGB1 in nuclear speckles. AtRBM22 also interacted with a nuclear transport factor, Ntf2, and a putative transcription factor, RBE, in nuclear speckles, which suggest that translocation of AtRBM22 into nuclear speckle is mediated by multiple proteins.

2.2 Introduction

The completed nucleotide sequence of the human genome revealed there are around 30,000 different genes in human genome (Lander *et al*., 2001; Venter *et al*., 2001). The gene number is below the amount of different proteins identified in cells. The high degree of proteomic complexity is realized due to the fact that one gene can generate structurally and functionally distinct protein isoforms as a result of alternative splicing (Graveley, 2001; Black and Grabowski, 2003).

2.2.1 Precursor-mRNA (pre-mRNA) splicing

The generation of mature messenger RNAs (mRNAs) from pre-mRNAs (or named as primary transcripts) requires the removal of noncoding sequences (introns) and splicing of the coding regions (exons; Labadorf *et al*., 2010). The exons are interrupted by introns in most eukaryotic genes. During some pre-mRNAs splicing, the same splice sites are used. This kind of processing was referred to constitutive splicing (CS), which results in a single transcript from one gene. In contrast, multiple mature mRNAs are generated from a single gene by alternative splicing (AS), where different combinations of splice sites are used in the pre-mRNAs processing.

Both CS and AS are critical for the expression of intron-containing genes. However, AS is a dominant property of higher organisms (Black, 2003; Blencowe, 2006). It has been calculated that more than 40% up to 42% of Arabidopsis (Filichkin *et al*., 2010), about 48% of rice (Lu *et al*., 2010), more than 40% of Drosophila (Stolc *et al*., 2004) and over two thirds of mouse genes (Johnson *et al*., 2003) give rise to alternatively spliced pre-mRNAs, whereas about 95% of human genes are alternatively spliced (Pan *et al*., 2008). Generally, in order to regulate the content of exons of a given mature mRNA thereby influencing the function of the encoded

protein in a specific cellular environment, AS processing permits fluctuation in the precise pairing of the splice sites thus generating alternative protein products. However, the AS regulation is still poorly understood.

2.2.2 Splicing factors

pre-mRNA splicing is catalyzed in a large complex named as spliceosome. In higher eukaryotes, there are two types of spliceosomes, the major (U2-type, containing U1, U2, U4, U5, and U6 snRNPs) and minor (U12-type, containing U11, U12, U4, U5, and U6atac) spliceosomes (Lorković *et al*., 2005; Ru *et al*., 2008). snRNPs is the shortened form of small nuclear ribonucleoproteins. In addition, spliceosomes are assembled not only by snRNPs but other protein factors, many of which are involved in the regulation of splicing (Wahl *et al*., 2009; Valadkhan and Jaladat, 2010). These splicing factors preferentially associated with nuclear structures designated as nuclear speckles, perichromatin fibrils, interchromatin granules, and coiled bodies (Spector *et al*., 1983; Fakan *et al*., 1984; Reuter *et al*., 1984; Puvion *et al*., 1984).

2.2.3 Nuclear speckles

Nuclear speckles were located in the interchromatin space and detected as a storage place for splicing factors (Fang *et al*., 2004; Spector and Lamond, 2012). Nuclear speckles contain snRNPs, non-snRNP splicing proteins, transcription factors, and 3’ end processing factors. pre-mRNAs were detected outside the speckles in fibrillar structures (Spector and Lamond, 2012). Hence, nuclear speckles observed near active transcription sites were viewed as storage and assembly of splicing factors. Nuclear speckles and their components are dynamic structures. They changed in size, in shape and in number. There is a hypothesis that actively transcribing cells have

smaller and more speckles, whereas inhibition of transcription or splicing leads to an accumulation of splicing factors and larger speckles.

In this study, we identified a putative pre-mRNA splicing factor AtRBM22 as a novel interacting partner of Arabidopsis G protein β subunits (AGB1) using yeast two-hybrid (Y2H) screening. RBM22 protein containing a CCCH-type zinc finger and a conserved RNA binding Motif (RBM) is highly conserved among invertebrates and vertebrates (Hartmuth *et al*., 2002; Rappsilber *et al*., 2002). It was found that human RBM22 (hRBM22) distributed evenly in the nucleus in NIH3T3 cells, and a mutant of hRBM22, replacing K170 and K324 by R, seem to accumulate in nuclear speckles (Krebs, 2009). In the presence of hRBM22, a cytosolic Ca^{2+}-binding protein ALG-2 became translocated to the nucleus, and the formation of complexes between ALG-2 and hRBM22 played a role in Ca^{2+} dependent signaling, which also influenced pre-mRNA splicing (Janowicz *et al*., 2011; Montaville *et al*., 2006). hRBM22 enhanced the cytoplasmic translocation of a spliceosomal nuclear protein hSlu7 under stress (Janowicz *et al*., 2011). RBM22 was required for embryos development of zebrafish (*Danio rerio*) by regulating the pre-mRNA splicing (He *et al*., 2009). A homolog of RBM22 was found in yeast (*Saccharomyces cerevisiae*, Slt11), which was identified as a pre-mRNA splicing factor involved in the activation and the assembly of the spliceosome (Xu and Friesen, 2001).

In Arabidopsis, AtRBM22 had been identified as a component of a nuclear protein complex MAC (MOS4 Associated Complex) and also known as MAC5A (Monaghan *et al*., 2009; 2010). MAC is a highly conserved spliceosome-associated complex homologous to yeast PRP19 complex (NTC) and human CDC5L complex (Tarn *et al*., 1994; Ajuh *et al*., 2000). In this study, AtRBM22 was identified as a novel target of Gβ subunit (AGB1). As a nuclear protein, AtRBM22 interacted with multiple proteins including AGB1 in nuclear spackles. The region of AtRBM22 which acted as a putative nuclear speckle localization signaling was identified.

2.3 Materials and methods

2.3.1 Plant materials and growth conditions

Arabidopsis thaliana Col-0 plants were used. AGB1-deficient mutant, *agb1-2*, was obtained from the Arabidopsis Biological Resource Center (ABRC, http://www.arabidopsis.org). Homozygous *agb1-2* was characterized as transcript-null mutant in the Col-0 background (Ullah *et al.*, 2003). Plants were grown at 22 ℃ under 8-h light/16-h dark condition (light intensity 120 μmol m^{-2} s^{-1}).

2.3.2 Yeast two-hybrid (Y2H) assay

Y2H experiments were performed using a Matchmaker Two-Hybrid System (Clontech). A cDNA library for the Y2H screen was prepared from mRNA samples from Arabidopsis mature leaves, using a Matchmaker Library Construction & Screening Kit (Clontech).

Full-length cDNA clone of *AGB1* (*AT4G34460*, RAFL05-19-B08) was obtained from RIKEN BRC Experimental Plant Division (Seki *et al.*, 2002). Full-length cDNA of *AGG2* (At3g22942), *AtRBM22* (At1g07360), *F16P2.4* (AT2G29580), *MOJ9.23* (AT5G07060), *Ntf2* (AT5G60980) and *RBE* (AT5G06070) were ordered from ABRC and used as PCR templates for following plasmids construction. The primers used in this part were shown in Table 2-1. The open reading frame (ORF) of *AGB1* was amplified by using primer pair with *Nde*I and *Sal*I sites. The PCR products were digested by *Nde*I and *Sal*I and cloned into the *Nde*I/*Sal*I site of pGBKT7 vector, generating pGBK-*AGB1*. This plasmid was used as the bait for Y2H. The ORF of *AtRBM22* was cloned into the *Sma*I/*Nde*I site of pGBKT7 and pGADT7-rec vector,

generating pGBK-*AtRBM22* and pGAD-*AtRBM22,* respectively. The ORF of *F16P2.4* and *MOJ9.23* were cloned into the *Eco*RI/*Sma*I site of pGADT7-rec vector, generating pGAD-*F16P2.4* and pGAD-*MOJ9.23.* The ORF of *AtPP2C52* (AT4G03415) was amplified by PCR using the cDNA cloned as template and cloned into the *Eco*RI/*Xba*I site of pGADT7-rec, generating pGAD-*AtPP2C52*. Pictures were taken after yeast cells cultured for 3-5 days. Yeast transformation using yeast strain AH109 and screening were performed by Matchmaker Gold Yeast Two-Hybrid System **(**Clontech**).**

2.3.3 *In vitro* Coimmunoprecipitation (Co-IP)

Proteins were expressed by TNT Quick Coupled Transcription/Translation Systems **(**Promega**).** Plasmid DNA pGBK-*AGB1,* pGAD-*AtRBM22* and pGADT7-rec vector were used to synthesize proteins Myc-tagged AGB1, HA-tagged AtRBM22 and HA epitope tag, respectively. Co-IP was carried out using anti-HA antibody **(**MBL), anti-Myc antibody **(**MBL) and protein G Sepharose **(**GE Healthcare) following the MATCHMAKER Co-IP Kit User Manual **(**Cat No. 630449, 2003**)**.

2.3.4 Localization studies

The vectors for Bimolecular Fluorescence Complementation (BiFC) assay were constructed by replacing GFP in the vector pBS-35SMCS:GFP (Tsugama *et al*., 2012) with the N-terminus (154 amino acids) or the C-terminus (80 amino acids) of YFP, generating pBS-35SMCS-nYFP and pBS-35SMCS-cYFP, respectively. The open reading frames (ORF) of *AGB1*, *Ntf2* and *RBE* without stop codon were amplified by using primer pair with *Kpn*I and *Spe*I sites. pBS-35SMCS-nYFP were created using a *Kpn*I/*Spe*I digestion to allow the insertion of the appropriate *AGB1, Ntf2* and *RBE*. Similarly, full length *AtRBM22, F16P2.4* and *MOJ9.23* without stop codon, and

deletion mutants of *AtRBM22* were cloned into *Kpn*I/*Spe*I site of pBS-35SMCS-cYFP and pBS-35SMCS:GFP. By this way, nYFP, cYFP and GFP-tag were fused to the C-terminus of these proteins. For co-expression *AGB1* with *AtRBM22:GFP*, the ORF of AGB1 was cloned into *Kpn*I/*Sac*I site of pBS-35SMCS:GFP generating pBS-35S-AGB1 without GFP. Arabidopsis protoplasts isolation and transformation were conducted as described (Wu *et al*., 2009). Plasmids DNA were introduced into onion epidermal cells by a bombardment system (Bio Red, PDS-1000). Images were processed using Canvas X software (ACD Systems). The diameter of nucleus and cell of protoplasts was measured by software ImageJ (http://rsbweb.nih.gov/ij/), and used for calculating the N/C ratio.

Table 2-1 Sequence of primer pairs.

Gene name	Primer name	Primer sequence
AGB1	F *EcoR*I	5’-GAGTCGAATTCATGTCTGTCTCCGAGCTC-3’
	R *BamH*I	5’-GAGTCGGATCCTCAAATCACTCTCCTGTG-3’
	R SacI	5’-GAGTCGAGCTCTCAAATCACTCTCCTGTG-3’
	F *Kpn*I	5’-GAGTCGGTACCATGTCTGTCTCCGAGCTC-3’
	R *Spe*I	5’-GAGTCACTAGTAATCACTCTCCTGTGTCCTCC-3’
	F *Nde*I	5’-CGCCATATGTCTGTCTCCGAGCTC-3’
	R *Sal*I	5’-CCCGTCGACAATCACTCTCCTGGTCCTCC-3’
AGG1	F *Not*I	5’-GATGAGCGGCCGCATGCGAGAGGAAACTGTGGTTTACG-3’
	R *Bgl*II	5’-GAGTCAGATCTAAGTATTAAGCATCTGCAGCCTTC-3’
AGG2	F *Not*I	5’-GATGAGCGGCCGCATGGAAGCGGGTAGCTCCAATTCGTC-3’
	R *BGI*II	5’-GAGTCAGATCTTCAAAGAATGGAGCAGCCACATCGTTTTGC-3’
AtRBM22	F *Sma*I	5’-GAGTCCCCGGGATGGCTCACAGAATAC-3’
	R NdeI	5’-GAGTCCATATGCTACTGAGACGAACCAG-3’
	F *Kpn*I	5’-GAGTCGGTACCATGGCTCACAGAATAC-3’
	R *Spe*I	5’-GAGTCACTAGTCTACTGAGACGAACCAG-3’
AtRBM22Δ 261	R *Spe*I	5’-GAGTC ACTAGTGGCCAAGATTCTGATAGATTCAA-3’
AtRBM22Δ 301	R *Spe*I	5’-GAGTC ACTAGTGGGTCTTCCCCATGTGAGTTTTAG-3’
AtRBM22Δ 331	R *Spe*I	5’-GAGTCACTAGTTTGATTGTGCTGCTGAGATATAACG-3’
AtRBM22Δ 366	R *Spe*I	5’-GAGTCACTAGTGGTTGAAATGACTGCACCCATTC-3’
AtRBM22Δ 399	R *Spe*I	5’-GAGTCACTAGTATATCCATATGGTGGTGGTGGGT-3’
Ntf2	F *Kpn*I	5’-GAGTCGGTACCATGGCACAGCAGGAAGCTAGTCC-3’
	R *Spe*I	5’-GAGTCACTAGTAGATGAACCACCACCTCGAG-3’
RBE	F *Kpn*I	5’-GAGTCGGTACCATGATGGATAGAGGAGAATGCTTG-3’
	R *Spe*I	5’- GAGTCACTAGTGTTAACCTTAGGCGGATCAGCTCC-3’
F16P2.4	F *Kpn*I	5’-GAGTCGGTACCATGGCGCATAGAATACTGAGAGATC-3’
	R *Spe*I	5’-GAGTCACTAGTTTGAGACGAACCAGTAGTAACAGC-3’
	F *EcoR*I	5’-GAGTCGAATTCATGGCGCATAGAATACTGAGAG-3’
	*R Sma*I	5’-GAGTCCCCGGGCTATTGAGACGAACCAGTAGTAAC-3’
MOJ9.23	F *Kpn*I	5’- GAGTCGGTACCATGTCTCACAGGGATCATGGAG-3’
	R *Spe*I	5’-GAGTCACTAGTTATATATATATATATATATCTATATATGGTGGTG-3’
	F *EcoR*I	5’-GAGTCGAATTCATGTCTCACAGGGATCATGGAG-3’
	R *Sma*I	5’-GAGTCCCCGGGTCATATATATATATATATATATCTATATATGGTGGTG-3’

Note: Digestion site corresponding to enzyme name was underlined. F, Forward primer. R, Reverse primer.

2.4 Results

2.4.1 AtRBM22 interacts with AGB1

Full-length AGB1 was used as the bait in the Y2H screen of the Arabidopsis leaf library. Even on high-stringency selection media, which lack histidine and adenine, more than 3600 positive clones were obtained. Yeast colony PCR with an AGG1-specific primer revealed that 60–70% of these clones expressed AGG1. Plasmid inserts from non-AGG1 clones were amplified by yeast colony PCR using a vector-specific primer pair and sequenced. Approximately 400 clones were examined and three of them were a conserved pre-mRNA splicing factor, AtRBM22 (GenBank Accession No. NP_563788). The physical interaction between AGB1 and AtRBM22 was confirmed using Y2H (Fig. 2-1A).

Coimmunoprecipitation (Co-IP) was used to determine whether AtRBM22 interacted with AGB1 *in vitro* (Fig. 2-1B). Myc-tagged AGB1 **(**Myc:AGB1**)**, HA-tagged AtRBM22 **(**HA:AtRBM22) and HA epitope tag **(**HA) were synthesized *in vitro* in a rabbit reticulocyte lysate system. Either HA epitope tag or HA:AtRBM22 were mixed with Myc-AGB1, and then precipitated by anti-HA antibody. Subsequently, G Sepharose was added. After incubation, Myc:AGB1 in the elutant from the G Sepharose was analyzed by immunoblotting using anti-Myc antibody. Specific signals of Myc:AGB1 were detected only when AtRBM22 was present (Fig. 2-1B), indicating that AtRBM22 interacts with AGB1 *in vitro*.

The interaction between AGB1 and AtRBM22 was confirmed with a BiFC assay (Fig. 2-1C,D). The N-terminal domain of YFP was fused to the N-terminus AGB1, while the C-terminal domains of YFP was fused to the C-terminus AtRBM22. Subsequently, both of them were co-introduced into Arabidopsis (Col-0) protoplasts and onion epidermal cells. Fluorescence from the reconstituted YFP was observed in a

speckled pattern in the nuclei of both Arabidopsis protoplasts (Fig. 2-1C) and onion epidermal cells (Fig. 2-1D). These fluorescent speckles appear to be the same as the nuclear speckles shown by Krebs (2009).

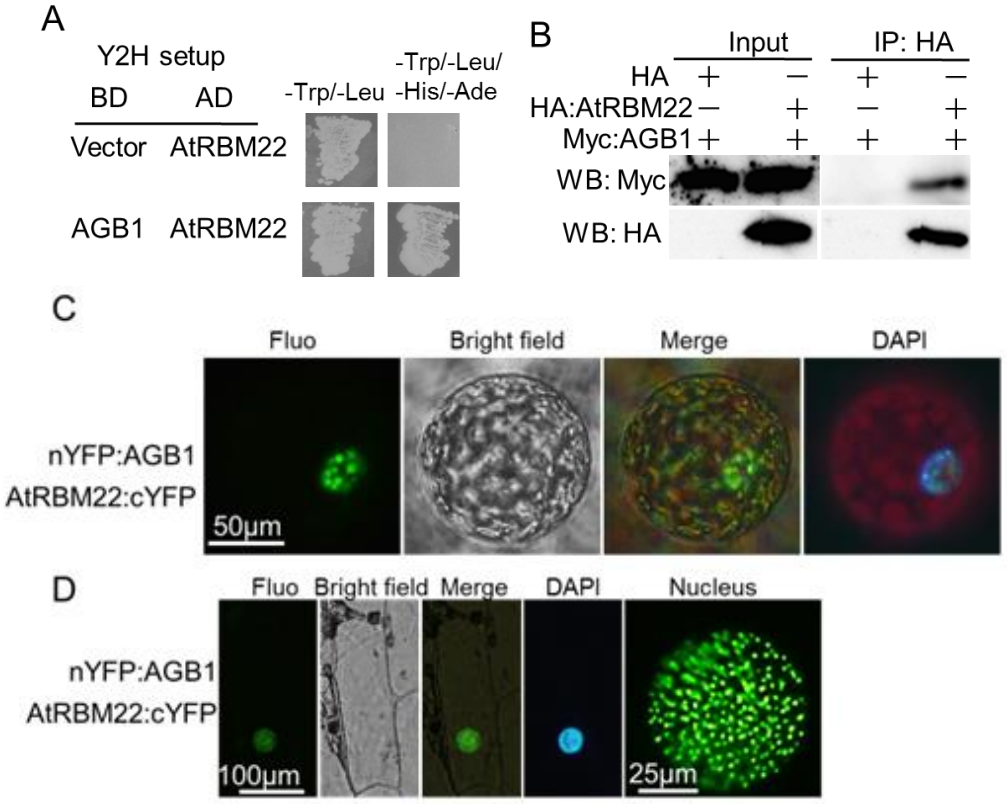

Fig. 2-1. Interaction between AtRBM22 and AGB1. A, Y2H analysis. In yeast cells that grew on quadruple dropout medium (SD/-Ade/-His/-Leu/-Trp), the reporter genes were activated when the bait (BD:AGB1) interacted with the prey (AD:AtRBM22). The combination of pGBKT7 vector (BD:vector) with AD:AtRBM22 is shown as a negative control. B. Co-IP. HA epitope tag and HA-tagged AtRBM22 (HA:AtRBM22) were immunoprecipitated with anti-HA antibody. Western-blot using anti-Myc antibody revealed that anti-HA antibody co-precipitated with Myc -tagged AGB1 (Myc:AGB1) in the presence of HA:AtRBM22 but not in the presence of HA epitope tag. C and D, BiFC assays in Arabidopsis protoplasts and onion epidermal cells, respectively. To visualize the nucleus, cells were stained by 4',6-diamidino-2-phenylindole (DAPI). The nucleus in E is enlarged at the right. Fluo: fluorescence from YFP or GFP. Merge: overlap of Bright field and Fluo signal.

2.4.2 AtRBM22 has a dynamic subcellular localization pattern

To check the subnuclear localization of AtRBM22, Green Fluorescent Protein (GFP)-tagged AtRBM22 was transiently expressed under control of the constitutive Cauliflower Mosaic Virus 35S (CaMV35S) promoter in Arabidopsis protoplasts. Consistent with a previous report, AtRBM22:GFP fusion protein was predominantly located in the nucleus (Fig. 2-2A e-l) (Monaghan *et al*., 2010), while GFP alone displayed fluorescence throughout the cytoplasm and nucleus (Fig. 2-2A a-d). Interestingly, two patterns of fluorescence were observed in protoplasts carrying the *AtRBM22:GFP* fusion gene: (i) evenly in the nucleus (Fig. 2-2A e) and (ii) in nuclear speckles (Fig. 2-2A i). The nuclear size of protoplasts with fluorescence pattern ii (N/C ratio: up to 0.12) was significantly larger than that of protoplasts with fluorescence pattern i (N/C ratio: around 0.06) (Fig. 2-2B, Fig. 2-3). When the *AGB1* gene and the *AtRBM22:GFP* fusion gene were co-introduced into the protoplasts, nearly 60% of the protoplasts had fluorescence pattern ii, while when only *AtRBM22:GFP* was introduced, only 38% of the protoplasts had fluorescence pattern ii (Fig. 2-2C). These results suggest that AGB1 has a role to promote the translocation of AtRBM22 into the nuclear speckles.

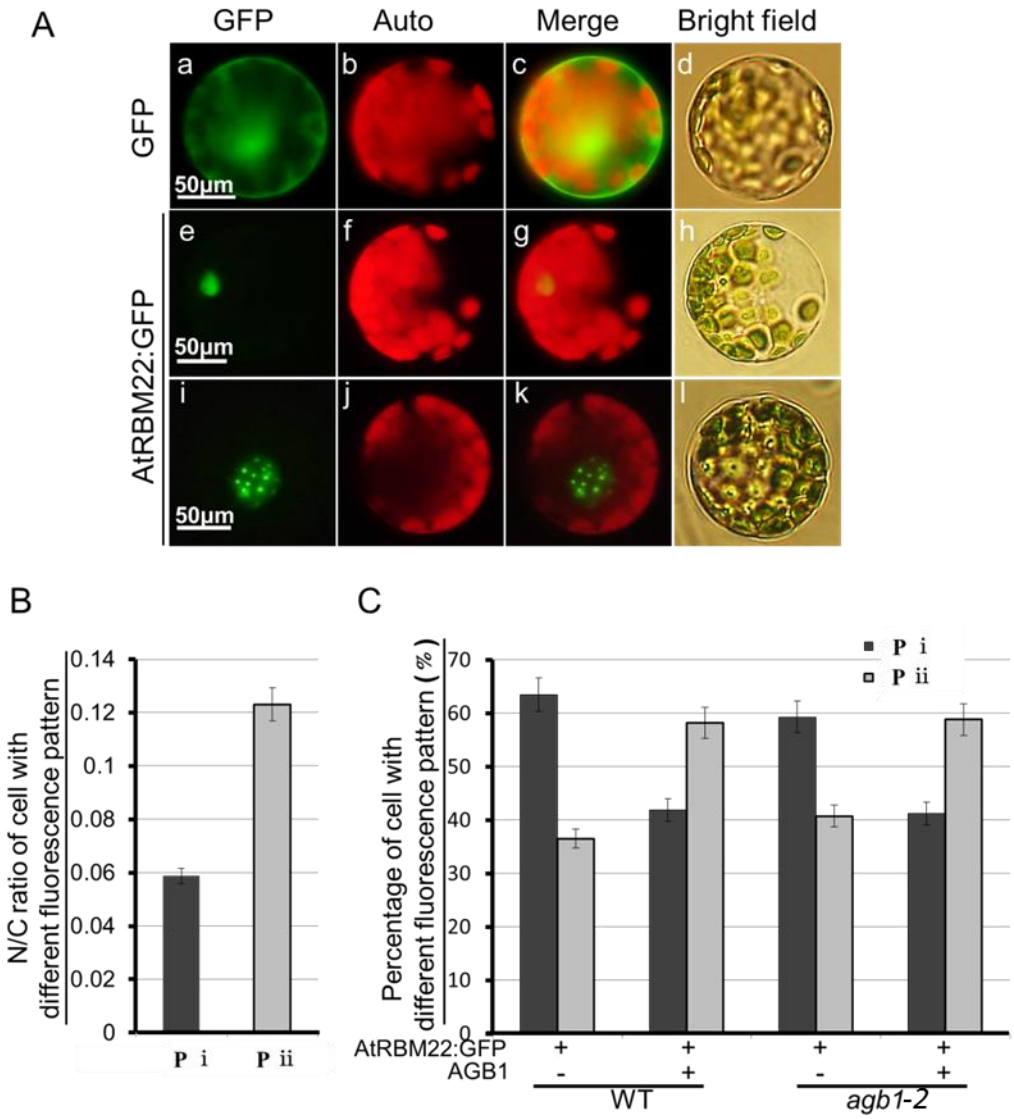

Fig. 2-2. Localization of AtRBM22 in the nucleus. A, Localization of AtRBM22 in Arabidopsis protoplasts. Fluo: fluorescence from YFP or GFP. Auto, chlorophyll. Merge: overlap of chlorophyll and Fluo signal. B, Comparison of the ratio of nuclear volume to cell volume (N/C ratio) of protoplasts with fluorescence pattern i (Pi) and pattern ii (Pii). More than 40 positive transfected cells with each florescence pattern were analyzed by ImageJ. The measurements were repeated three times. C, In the background of wild-type and *agb1* null mutants (*agb1-2*), percentages of Pattern i (Pi) and Pattern ii (Pii) in Arabidopsis protoplasts carrying *AtRBM22:GFP* alone and carrying *AtRBM22:GFP* and *AGB1* were compared. More than 200 positive transfected cells of each line were examined. Experiments were performed in triplicate. Values are means ±SE.

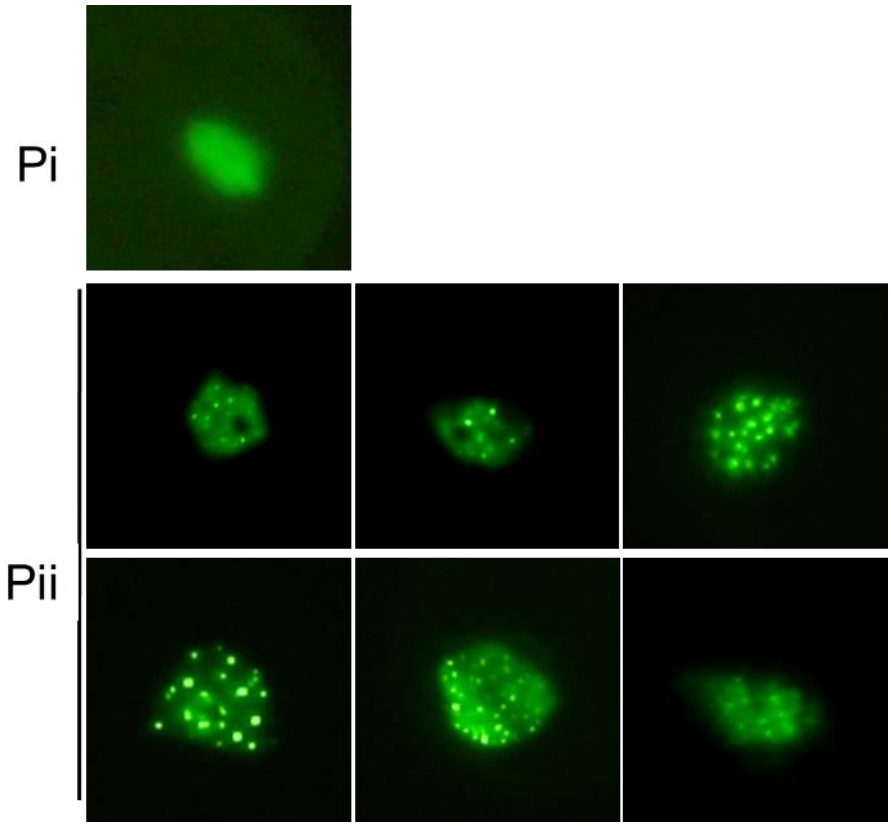

Fig. 2-3. The nuclear shapes of protoplasts with florescence pattern ii (P ii) varied, and were different from the shape of protoplasts with florescence pattern i (Pi). The pictures were taken without changing any parameters of the microscope.

In onion epidermal cells, the fluorescence of AtRBM22:GFP fusion protein was evenly diffused in the nucleus (Fig. 2-4 g-j). AGB1:GFP fusion protein was located in the plasma membrane and nucleus as described previously (Fig. 2-4 d-f) (Chen *et al*., 2006; Anderson and Botella, 2007). When *AGB1* and *AtRBM22:GFP* fusion gene were co-introduced into onion epidermal cells, the fluorescence of AtRBM22:GFP fusion protein was diffused in the nucleus, and speckle-like structures were visible in the nuclei of almost all cells (Fig. 2-4 k-n). These results indicate that the localization of AtRBM22 in nuclear speckles in Arabidopsis protoplasts is not due to the high expression level of AtRBM22 and suggest that the translocation of AtRBM22 to nuclear speckles in onion epidermal cells requires AGB1.

To confirm whether the wild type (WT) protoplasts with fluorescence pattern ii depended on the presence of endogenous AGB1, *agb1* null mutant (*agb1-2*) was used to check the localization of AtRBM22:GFP fusion protein. Similarly, both patterns of fluorescence were observed from *agb1-2* protoplasts carrying *AtRBM22:GFP* fusion gene only (data not shown). The percentages of *agb1-2* protoplasts with both fluorescence patterns were equal to that of WT when either only *AtRBM22:GFP* was introduced or both *AGB1* gene and the *AtRBM22:GFP* fusion gene were co-introduced (Fig. 2-2C). These results raise the possibility that proteins other than AGB1 also mediated the translocation of AtRBM22 to nuclear speckles.

In another Y2H screening using full-length AtRBM22 as the bait, Ntf2 and RBE (GenBank Accession Nos. NP_851235 and NP_568161) were identified as AtRBM22 interactors from more than 3000 positive clones. Among the 250 clones examined, three encoded a RBM motif containing protein Ntf2 (NP_851235.1) and two encoded a putative transcriptional regulator *RBE* (NP_568161.1, data not shown). Ntf2 is a dedicated nuclear import factor to recycle Ran-GDP from the cytoplasm to the nucleus (reviewd by Stewart, 2000). Ntf2 was diffused in cytoplasm and nucleocytoplasm (Fig. 2-5 a-d). RBE which has been identified as a regulator of petal

development by restricting *AGAMOUS* expression in Arabidopsis (Krizek *et al*., 2006) was localized in the nucleus (Fig. 2-5 i-l). Both Ntf2 and RBE interacted with AtRBM22 in the nucleus speckles as shown in BiFC assay (Fig. 2-5 e-h, m-p). These results suggest that translocation of AtRBM22 into nuclear speckles is mediated by multiple proteins.

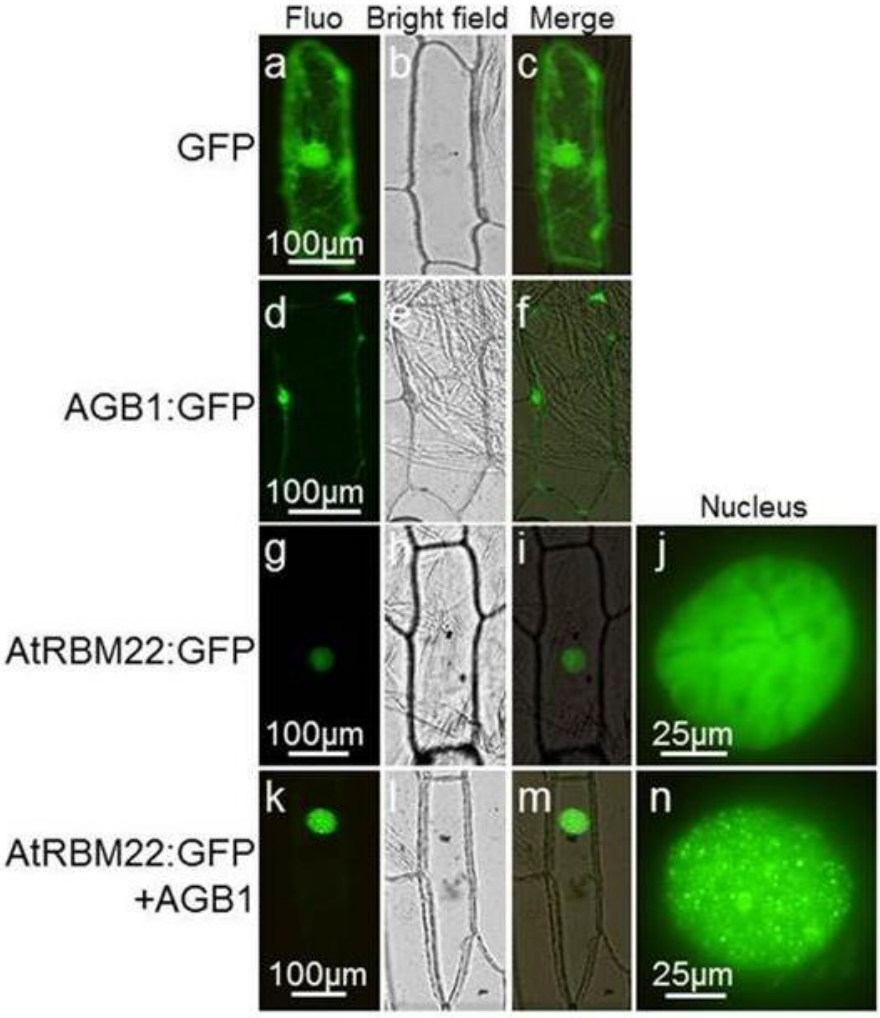

Fig. 2-4. AGB1 enhanced the translocation of AtRBM22:GFP to nuclear speckles. The nucleus is enlarged at the right. Fluo: fluorescence from YFP or GFP. Merge: overlap of Bright field and Fluo signal.

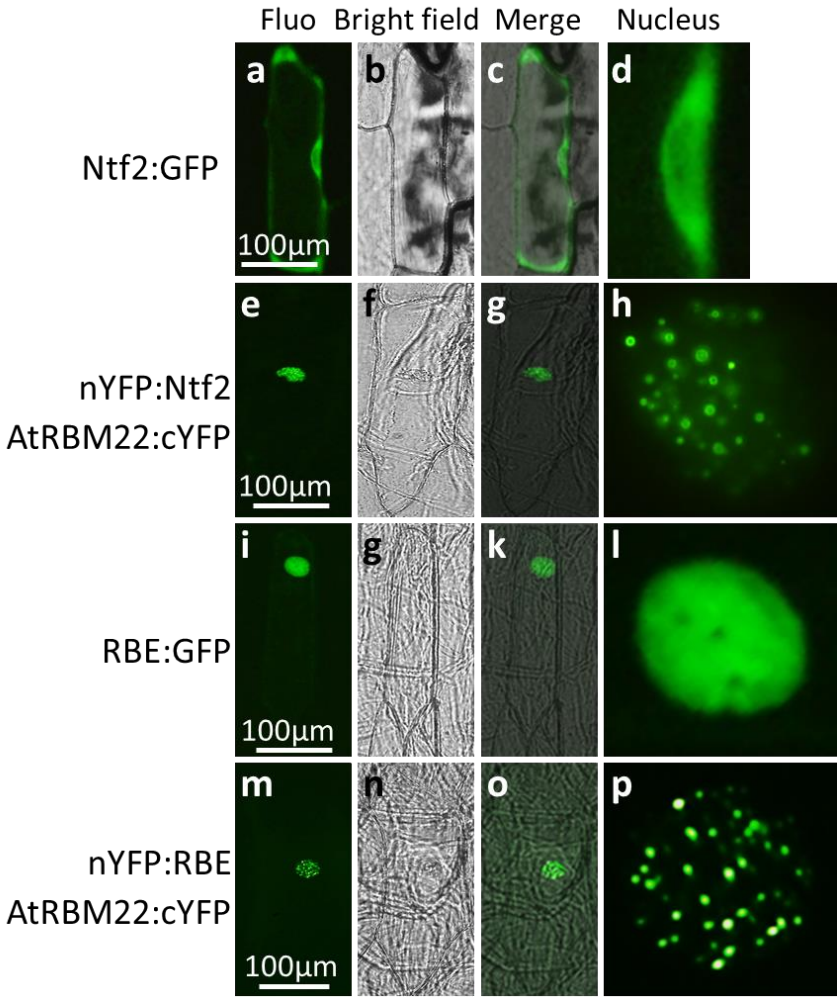

Fig. 2-5. AtRBM22 interacted with Ntf2 and RBE in nuclear speckles. Ntf2 was an intracellular protein (a-d). d, the enlarged view indicated by a white rectangle in a. BiFC of AtRBM22 and Ntf2 (e-h). BiFC of AtRBM22 and RBE (m-p). The nuclei are enlarged at the right. Fluo: fluorescence from YFP or GFP. Merge: overlap of Bright field and Fluo signal.

2.4.3 Signaling domain of AtRBM22 for localization in nuclear speckles

The amino acid sequence of RBM22 proteins were analyzed (Table 2-2, Fig. 2-6) RBM22 proteins contain a C-x8-C-x5-C-x3-H zinc finger motif and a conserved RNA Binding Motif (RBM). Two RBM22 homologues of Arabidopsis, F16P2.4 and MOJ9.23 (GenBank Accession Nos. NP_180518 and NP_196323) share 86.8% and 71.3% identity with AtRBM22, respectively. AtRBM22 shares 70.7% and 73.5% identity with two homologues in *O. sativa*, respectively. AtRBM22 shares approximately 50% identity with RBM22 homologues from *H. sapiens*, *D. rerio*, *D. melanogaster* and *C. elegans*.

F16P2.4, which shares high similarity with AtRBM22, was localized in nuclear speckles in onion epidermal cells without ectopic expression of AGB1 (Fig. 2-7 a-d). Fluorescence from BiFC of AGB1 and F16P2.4 was observed in nuclear speckles in onion epidermal cells (Fig. 2-7 i-l). On the other hand, MOJ9.23:GFP fusion protein was evenly diffused in the nucleus (Fig. 2-7 e-h). BiFC fluorescence of AGB1 and MOJ9.23 was weak and was observed in the plasma membrane and nucleus (Fig. 2-7 m-o), which was possibly a result of both proteins being in close proximity but not close enough to interact directly. Consistently, MOJ9.23 failed to interact with AGB1 in Y2H, while F16P2.4 had Y2H interaction with AGB1 (Fig. 2-7B). These results suggest that AtRBM22 and its close homologue F16P2.4 were associated with nuclear speckles and have specifically interaction with AGB1 in yeast.

Table 2-2 Analysis of the amino acid sequences of RBM22 from various species.

Species	Locus	C-x8-C-x5-C-x3-H	RBM	Full length protein	
		Region	Region	Length (aa)	Identity (%)
Arabidopsis thaliana	NP_563788	157-181	229-298	481	100
	NP_180518	157-181	229-298	483	86.8
	NP_196323	154-178	226-257	363	71.3
Oryza sativa Japonica	NP_001059374	157-181	229-298	486	73.5
	NP_001056931	157-181	229-298	482	70.7
Homo sapiens	NP_060517	159-185	233-302	420	51
Danio rerio	NP_998379	159-185	233-302	425	49.9
Drosophila melanogaster	NP_649440	159-185	233-302	418	48.6
Caenorhabditis elegans	NP_502014	165-188	236-309	408	51.2

Note: Zinc finger domain type, C-x8-C-x5-C-x3-H. RNA Binding Motif, RBM. Amino Acid, aa.

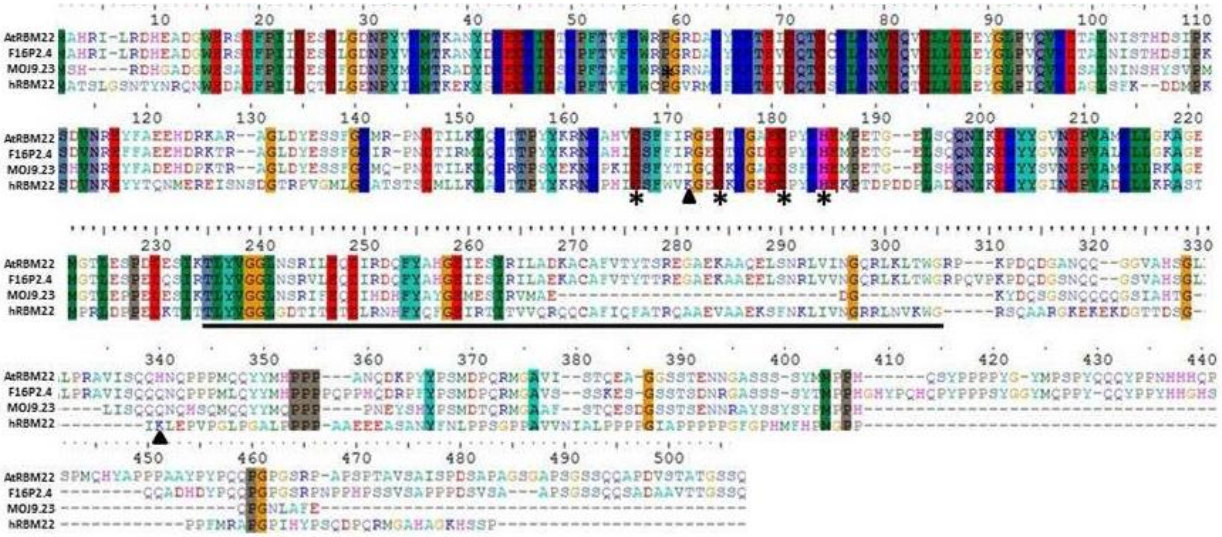

Fig. 2-6. Comparison of amino acid sequences of human RBM22 (hRBM22) with RBM22 homologues in Arabidopsis. hRBM22 (NP_060517), AtRBM22 (NP_563788), F16P2.4 (NP_180518) and MOJ9.23 (NP_196323). A conserved C-x8-C-x5-C-x3-H zinc finger is indicated by asterisks. A conserved RBM is underlined. The two sumoylation sites (Lys 170 and Lys 324) of hRBM22 were indicated by black triangles.

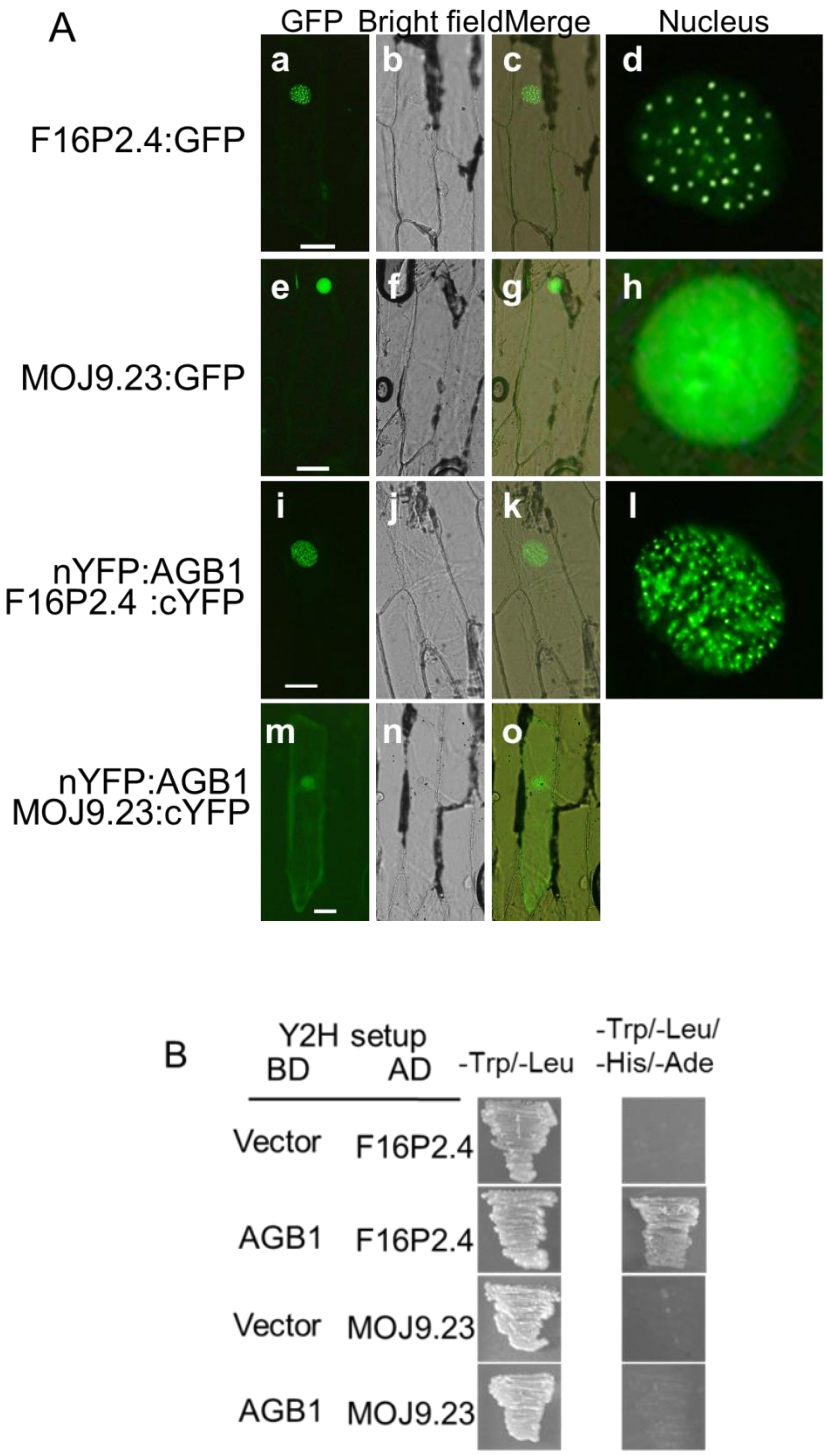

Fig. 2-7. AGB1 interacted with F16P2.4 in nuclear speckles. A, The nuclei are enlarged at the right. Fluo: fluorescence from YFP or GFP. Merge: overlap of Bright field and Fluo signal. Bar=100μm. B, In yeast cells that grew on quadruple dropout medium (SD/-Trp/-Leu/-His/-Ade), the reporter genes were activated when the bait (BD:AGB1) interacted with the prey

(AD:F16P2.4). In yeast cells that failed to grow on quadruple dropout medium (SD/-Trp/-Leu/-His/-Ade), the reporter genes were not activated when the bait (BD:AGB1) could not interact with the prey (MOJ9.23). The combinations of pGBKT7 vector (BD:vector) with F16P2.4 or MOJ9.23 are shown as negative controls.

AtRBM22 is thought to have a subnuclear localization signal for the translocation to nuclear speckles. It was suspected that the signal was in the C-terminus region, where AtRBM22 and its homologues show a lot of divergence (Fig. 2-6). Thus, to identify the signal, a series of deletion mutants of AtRBM22 in the C-terminus domain were created (between residues 261 and 481, Fig. 2-8A). BiFC fluorescence of AtRBM22$^{\Delta C301}$ (residues 301 to 481 were deleted) and AGB1 was evenly diffused in the nucleus and failed to form speckle-like structures (Fig. 2-8B). BiFC fluorescence of AtRBM22$^{\Delta C331}$ (residues 331 to 481 were deleted) and AGB1 was observed in a speckled pattern (Fig. 2-8B) just as when full-length AtRBM22 was used (Fig. 2-1D). The Y2H interaction between AGB1 and AtRBM22 was not disturbed by the deletion (Fig. 2-8C). These results indicate that residues (301-331) of AtRBM22 act as a putative subnuclear localization signal for targeting to the nuclear speckles.

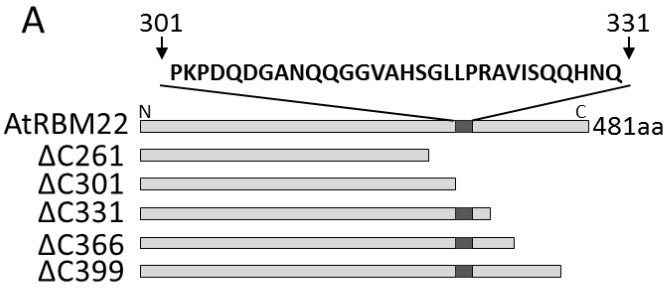
A
301
331
PKPDQDGANQQGGVAHSGLLPRAVISQQHNQ
N
C
AtRBM22
481aa
ΔC261
ΔC301
ΔC331
ΔC366
ΔC399

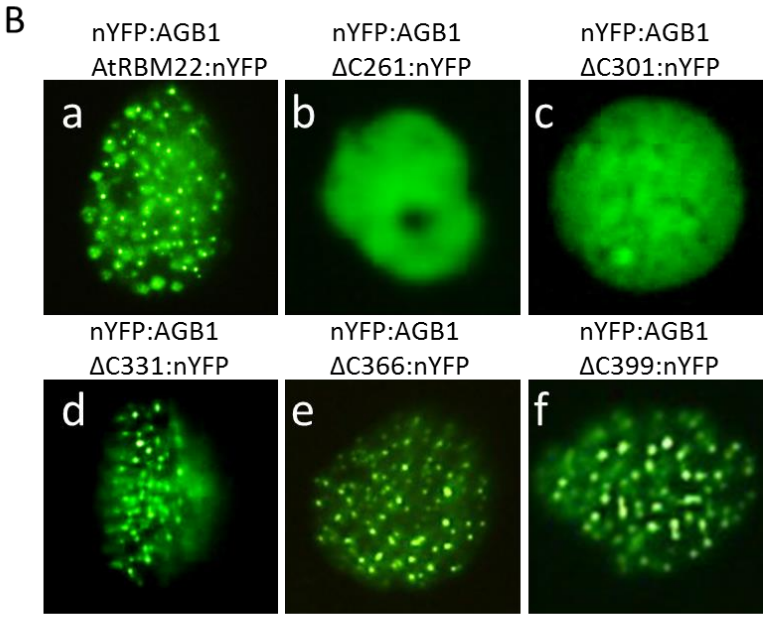
B
nYFP:AGB1
AtRBM22:nYFP
nYFP:AGB1
ΔC261:nYFP
nYFP:AGB1
ΔC301:nYFP
a
b
c
nYFP:AGB1
ΔC331:nYFP
nYFP:AGB1
ΔC366:nYFP
nYFP:AGB1
ΔC399:nYFP
d
e
f

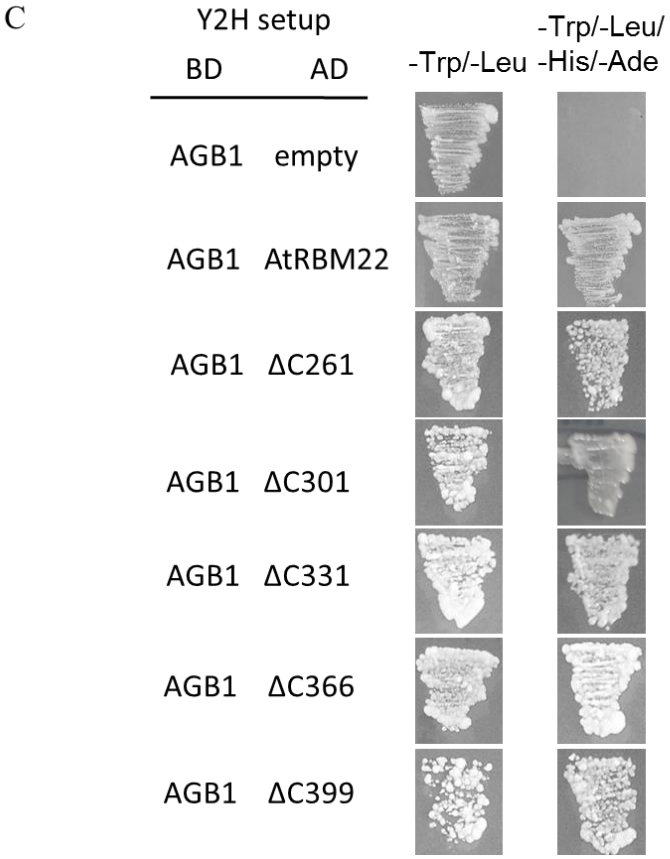
C
Y2H setup
BD
AD
-Trp/-Leu
-Trp/-Leu/
-His/-Ade
AGB1 empty
AGB1 AtRBM22
AGB1 ΔC261
AGB1 ΔC301
AGB1 ΔC331
AGB1 ΔC366
AGB1 ΔC399

Fig. 2-8. A putative nuclear speckles localization signal domain of AtRBM22. A, Schematics of truncated AtRBM22. B, BiFC assay of deleted mutants of AtRBM22 and AGB1 in onion epidermal cells. The nuclei were shown. C. Y2H assay of deleted mutants of AtRBM22 and AGB1.

2.5 Discussion

2.5.1 AtRBM22 is a novel AGB1-interacting protein

In this study, AtRBM22 was identified as a novel AGB1-interacting protein and was shown to interact with AGB1 in nuclear speckles (Fig. 2-1). AtRBM22 is a putative pre-mRNA splicing factor and shares around 50% identity with hRBM22 (Table 2-2). hRBM22 assisted nuclear translocation of a cytosolic Ca^{2+}-binding protein, ALG-2. The complexes between ALG-2 and hRBM22 played a role in Ca^{2+}-dependent signal transduction, which influenced pre-mRNA splicing (Montaville *et al*., 2006). We suggest that AtRBM22, which may be involved in pre-mRNA splicing, is an effector candidate of AGB1.

2.5.2 Localization of AtRBM22 in nuclear speckles

Protoplasts carrying *AtRBM22:GFP* fusion gene showed two patterns of fluorescence in the nucleus: evenly diffused fluorescence (pattern i, Fig. 2-2A e) and fluorescence in speckle-like structures (pattern ii, Fig. 2-2A i). In onion epidermal cells, AtRBM22:GFP fusion protein evenly diffused in the nucleus (Fig. 2-4 j). The speckled fluorescence in Arabidopsis protoplasts (Fig. 2-2A i) may be related to that the protoplasts were isolated in a highly osmotic solution. In response to osmotic stress, the endogenetic AGB1 or other proteins in certain protoplasts resulted in the translocation of AtRBM22 into nuclear speckles. Consistently, ectopic AGB1 expression led to the translocation of AtRBM22 into nuclear speckles in onion epidermal cells (Fig. 2-4 n). These results support that AGB1 played a role in the translocation of AtRBM22 into nuclear speckles and AtRBM22 may be involved in the signal transduction pathway mediated by AGB1. The residues 301-331 in AtRBM22 were required for the localization of AtRBM22-AGB1 complexes in

nuclear speckles (Fig. 2-8), suggesting that this region acts as a nuclear speckles signaling domain. Other regions or amino acids of AtRBM22 may be involved in nuclear speckle localization signals. F16P2.4, which shares high similarity with AtRBM22, was located in the nucleus and formed speckle-like structures without ectopic expression of AGB1 in onion epidermal cells (Fig. 2-7 d). In addition, a mutant of hRBM22 in which two sumoylation sites (Lys 170 and Lys 324) were replaced by Arg was reported to accumulate in speckle-like structures in the nucleus (Krebs, 2009), but the two sumoylation sites of hRBM22 were not conserved in RBM22 homologues of Arabidopsis (Fig. 2-6). Further studies are necessary to precisely identify the domains needed for nuclear speckles localization of AtRBM22.

2.5.3 AtRBM22 affects the nuclear size

In most eukaryotes, the nuclear volume and cell volume are highly correlated. In yeast, the N/C ratio was found to be 0.08, and was not affected by nitrogen starvation or changes in ploidy (Neumann and Nurse, 2007). The N/C ratio of Arabidopsis is also kept constant (Jovtchev *et al*., 2006). However, when AtRBM22:GFP fusion protein was introduced in Arabidopsis protoplasts, the N/C ratio of protoplasts with fluorescence pattern ii (Fig. 2-2A i, Fig. 2-3) was significantly larger than that of protoplasts with fluorescence pattern i (Fig. 2-2A e, Fig. 2-3). In eukaryotes, the size of the nucleus depends on the species, the cell type, and the disease state, but regulation of nuclear size is poorly understood.

A highly positive correlation was found between DNA content and nuclear volume (Jovtchev *et al.*, 2006). The cell doubles its DNA in preparation for undergoing mitosis. hRBM22 deficiency leads to culture cell death upon entry into mitosis, suggesting that hRBM22 is essential for cell division (Kitter *et al.*, 2004). RBM22 proteins from various species are highly conserved, and AtRBM22 shares high similarity with hRBM22 (Table 2-2, Fig 2-6). In Arabidopsis, the enlarged nuclei

may be a result of that AtRBM22 affects the cell division as well as hRBM22.

On the other hand, nuclear size was found to be correlated with the nuclear import rate, and the concentration of Ntf2 is one of the factors sufficient to account for nuclear scaling in *Xenopus laevis* (Levy and Heald, 2010). Ntf2 is a nuclear import factor that recycles Ran-GDP from the cytoplasm to the nucleus, and plays a role in decreasing nuclear size (Levy and Heald, 2010). In this study, AtRBM22 interacted with Ntf2 in nuclear speckles (Fig. 2-5 g). The enlarged nuclear size may relate to the disturbed balance of concentration of Ntf2 between the cytosol and the nucleocytoplasm.

In this study, a putative pre-mRNA splicing factor, AtRBM22, was identified as a novel AGB1-interacting protein. AtRBM22, which has a dynamic subcellular localization in nuclear speckles and nuclei, can interact with AGB1, Ntf2, and RBE in nuclear speckles. Further studies of the molecular function of AtRBM22 in Arabidopsis may lead to a better understanding of the function of pre-mRNA splicing factors.

Chapter 3

AtRBM22 has roles in the development of Arabidopsis

3.1 Abstract

RNA-binding proteins modulate the gene expression directly and indirectly. AtRBM22 protein contains one RBM domain and a CCCH-type zinc finger motif. GUS staining revealed that *AtRBM22* gene was specifically expressed in root tip of seedlings. In mature plant, *AtRBM22*-promoter GUS signal was observed in pollen. With the process of pollination, *AtRBM22*-promoter GUS signal was found in stigma and ovary. Phenotypic analysis of *atrbm22* null mutants shown that *atrbm22* mutation caused early flowering and shorter silique. The early flowering of *atrbm22* mutants may result from the decreased expression of a floral inhibitor FLC. In homozygous transgenic plants overexpressing *AtRBM22:GFP* fusion gene, the GFP fluorescence was observed only from guard cells. A serious dwarf phenotype and abnormal flowers morphology were shown in these transgenic plants. The expressions of auxin-responsive genes were changed in these transgenic plants. Exogenous overexpression of *AtRBM22* and *atrbm22* mutation resulted ABA insensitivity during germination. Plants overexpressing of AtRBM22 were sensitive to NaCl.

3.2 Introduction

In response to endogenous and environmental cues, shoot apical meristem (SAM) transits to an inflorescence meristem (IM) that is capable of producing floral meristems (FMs) in the reproductive development of Arabidopsis. The timing of floral transition is controlled by a multiple and redundant gene network. The floral transition ends with the initiation of flower development. Four major classes of homeotic genes, A, B, C and E, confer the four floral organs in a combinatorial manner (Krizek and Fletcher, 2005). Almost all of these homeotic genes are identified as MADS-domain transcriptional factors. Members of MADS-domain proteins interact not only with each other but also with non-MADS proteins, suggesting various specific combinatorial modes of action (Smaczniak *et al*., 2012).

Regulation of gene expression at post-transcriptional level is modulated by RNA-binding proteins either directly or indirectly (Burd and Dreyfuss, 1994; Lorković and Barta, 2002). The interaction of RNA binding protein and its substrate is determined by specific sequences within the RNA binding proteins, such as the RNA-binding motif (RBM), CCCH-type zinc fingers, C4-type zinc fingers, K homology (KH) domains, and so on (Lorković and Barta, 2002).

In Arabidopsis, the RNA-binding motif protein AtRBM22 (At1g07360), contains one RBM domain and a CCCH-type zinc finger motif. AtRBM22 have been identified as a component of a nuclear protein complex MAC (MOS4 Associated Complex) that contributes autoimmunity (Monaghan *et al.*, 2009, 2010). *atrbm22* knockout mutant plants were early flowering and shown changes in morphology of leaves and roots (Monaghan *et al*., 2010). Here, *AtRBM22* gene was predominantly expressed in pollen by GUS staining. Dwarf phenotype, abnormal flower phenotypes and reduced seed production were found in the AtRBM22 overexpressing plants. These results suggest that AtRBM22 plays multiple roles in Arabidopsis.

3.3 Materials and methods

3.3.1 Genetic stocks and growth conditions

Salk_132881 (*atrbm22*) mutant seed stocks used was in a Columbia (Col-0) genetic backgrounds, and was obtained from the Arabidopsis Biological Resource Centre (ABRC, http://www.arabidopsis.org). *atrbm22* mutant, which carries a T-DNA insertion in the second exon of *AtRBM22* gene, was isolated by PCR using the three primers listed in Table 3-1. Seeds were surface sterilized and plated on 0.5×MS salt (Wako) medium containing 0.8% agar, 1% w/v sucrose and 0.5g/l MES, PH 5.8. After sowing, plates were chilled for 72h at 4℃ in darkness and subsequently incubated at 22℃ under long day photoperiods (LDs) or short day photoperiods (SDs). LDs consist of 16-h light/8-h darkness; SDs consist of 8-h light/16-h. Light intensity is 120 μmol m^{-2} s^{-1}. After ten days of growth, plants were transferred onto rockwool cubes and grown further with 0.2×MS solution regularly supplied.

3.3.2 Preparation of chimeric constructs

To generate pBI121-$P_{AtRBM22}$::*GUS* construct, the CaMV 35S promoter of pBI121 vector (Clontech, Bevan, 1984) was replaced with a 2kb upstream promoter sequence of *AtRBM22* ($P_{AtRBM22}$) double-digested with *Spe*I/*Sma*I. Full length AtRBM22 without stop codon were cloned into *Kpn*I/*Spe*I site the vector pBS-35SMCS:GFP (Tsugama *et al*., 2012), generating pBS-35S::*AtRBM22:GFP*. A *AtRBM22:GFP* fusion gene was cloned from pBS-35S::*AtRBM22:GFP* by using primer pair with *Bam*HI and *Sac*I, *and* cloned into the pBI121 vector to replace the *GUS* gene, generating pBI121-35S::*AtRBM22:GFP*. Primers used were listed in Table 3-1. pBS-35SMCS:GFP were digested by *Xba*I and *Sac*I to obtain the open reading frame of (ORF) of GFP. The GFP fragments were inserted into the *Xba*I/*Sac*I site of

pBI121.

3.3.3 Plant transformation

Arabidopsis Col-0 plants were transformed by *Agrobacterium tumefaciens*-mediated transformation using the floral-dip method (Clough and Bent, 1998). The Agrobacterium strain used was EHA105 harboring binary vector pBI121 carrying the pBI121-35S::*AtRBM22:GFP* or pBI121-$P_{AtRBM22}$::*GUS*.

3.3.4 Germination and growth assay

Seeds were surface sterilized and plated on half-strength MS medium supplemented with or without ABA. After sowing, plates were chilled for 3 d at 4℃ in darkness and subsequently incubated at 22℃ under LDs or SDs. Emerging root tips were scored with the light microscope. Seeds of batches of exactly the same age were used for one experiment, but batches varied from one experiment to the next. For post-germination growth assay, 3-day-old seedlings were transferred to half-strength MS medium supplemented with or without NaCl.

3.3.5 Histochemical β-glucuronidase assays

Chlorophyll of $P_{AtRBM22}$::*GUS* plants was cleared through 90% acetone. GUS activity was revealed by incubation in 100 mM $NaPO_4$ (pH 7.2), 5 mM 5-bromo-4-chloro-3-indolyl-D-glucuronide, 0.5 mM $K_3Fe(CN)_6$, 0.5 mM $K_4Fe(CN)_6$ and 0.25% Triton X-100. Plant tissue was incubated at 37℃. After staining, sample was cleared through 70% ethanol.

3.3.6 Expression analysis

Total RNA was isolated with RNeasy Plant Mini Kit (QIAGEN). cDNA was

prepared using PrimeScript Reverse Transcriptase (TaKaRa). qRT-PCR was carried out using a StepOne Real-Time PCR System (Applied Biosystems) and the SYBR Premix Ex Taq (TaKaRa). Actin (NM_112764) levels were used to normalize expression patterns between samples. Primers used for qRT-PCR were listed in Table 3-1 and Table 3-2.

Table 3-1 Sequence of primer pairs.

Primer name	Primer sequence
LBb1.3	5′-ATTTTGCCGATTTCGGAAC-3′
LP	5′-AAAGACAAAAACACGCGAATC-3′
RP	5′-ATGGACATTCAGCACCTCTTG-3′
$P_{AtRBM22}$ Fw *Spe*I	5′-AGGGACTAGTTCTCTTATCCTCTGATTCG-3′
$P_{AtRBM22}$ Rv *Sma*I	5′-TACGCCCGGGCTTGTATTATACTAGGTTTACC-3′
AtRBM22 Fw *Kpn*I	5′-GAGTCGGTACCATGGCTCACAGAATAC-3′
AtRBM22 Rv *Spe*I	5′-GAGTCACTAGTCTACTGAGACGAACCAG-3′
AtRBM22 Fw *Bam*HI	5′-GAGTCGGATCCATGGCTCACAGAATAC-3′
GFP Rv *Sac*I	5′-GAGTAGAGCTCTTACTTGTACAGCTCGTCCATGCCG-3′
AtRBM22 qRT Fw	5′-GCAAGATATGTACACGACC-3′
AtRBM22 qRT Rv	5′-AGTGCCCATCTCACCAGCTT-3′

Table 3-2 Primer pairs used for qRT-PCR.

Gene name	Gene accession	Primer name	Primer sequence
GH3.5	At4g27260	qRT Fw	AGCCCTAACGAGACCATCCT
		qRT Rv	AAGCCATGGATGGTATGAGC
SAUR9	AT4G36110	qRT Fw	GACGTGCCAAAAGGTCACTT
		qRT Rv	AGTGAGACCCATCTCGTGCT
IAA19	At3g15540	qRT Fw	GGTGACAACTGCGAATACGTTACC
		qRT Rv	CCCGGTAGCATCCGATCTTTTCA
IAA5	AT1G15580	qRT Fw	AAGAGTCAAGTTGTGGGTTGGC
		qRT Rv	AATGCAGCTCCATCTACACTCACT
HAT2	AT5G47370	qRT Fw	CCCATCATCATCGAACCATC
		qRT Rv	AAACACCCTTTTCCCACCAC
LBD29	AT3G58190	qRT Fw	GCTAGGCTTCAAGATCCCATC
		qRT Rv	TGTGCTGCTTGTTGCTTTAGA
FLC	AT5G10140	qRT Fw	AGCCAAGAAGACCGAACTCA
		qRT Rv	TTTGTCCAGCAGGTGACATC
FT	AT1G65480	qRT Fw	CTGGAACAACCTTTGGCAAT
		qRT Rv	AGCCACTCTCCCTCTGACAA

Note: Digestion site corresponding to enzyme name was underlined.

3.4 Results

3.4.1 AtRBM22 is expressed in a tissue-specific manner

According to the publicly available microarray data (http://bar.utoronto.ca/efp_arabidopsis and http://bar.utoronto.ca/eplant), the expression of *AtRBM22* gene was higher in guard cell, shoot apex, pollen, carpel, young silique, and mature seed.

To confirm the temporal-spatial expression pattern of *AtRBM22*, transgenic plants expressing a promoter-reporter fusion gene ($P_{AtRBM22}$::*GUS*) were used. $P_{AtRBM22}$::*GUS* was expressed in a tissue-specific manner (Fig. 3-1). In young seedlings, $P_{AtRBM22}$::*GUS* was specifically expressed in root tips (Fig. 3-1A). In adult plants, $P_{AtRBM22}$::*GUS* was expressed in pollen but not in gynoecium in early flower stages (Fig. 3-1B b-d,f). In flower stage 14, $P_{AtRBM22}$::*GUS* signal was found in stigma and ovary (Fig. 3-1B e,g). In flower stage 15, $P_{AtRBM22}$::*GUS* signal was disappeared from anther (Fig. 3-1B h). These results indicate that *AtRBM22* is expressed in stigma and ovary with the process of pollination. $P_{AtRBM22}$::*GUS* was predominantly expressed in the sporangia of your silique (Fig. 3-1B i) and disappeared in mature silique (Fig. 3-1B j). $P_{AtRBM22}$::*GUS* signal was not detected in leaves and stem (Fig. 3-1B a). In mature plants, $P_{AtRBM22}$::*GUS* was specifically expressed flower pollen, indicating that *AtRBM22* is involved in the reproductive growth of plant.

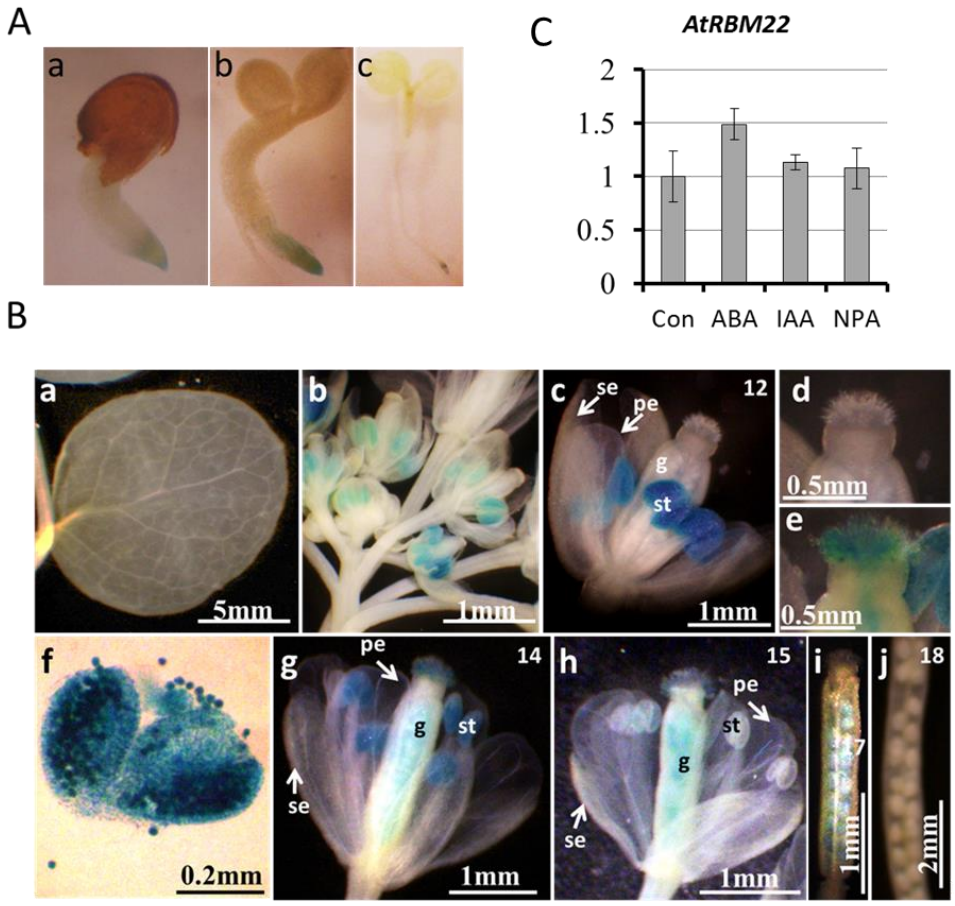

Fig. 3-1. Temporal and spatial expression of *AtRBM22*. A, GUS staining in seedlings, 1-3 day after germination. B, GUS staining in mature plant. a, No expression of $P_{AtRBM22}$:*GUS* in leaf. b, Inflorescence. c, Flower at stage 12. d, Stigma of flower at stage 12. e, Stigma of flower at stage 14. f, Anther. g and h, Flower at stage 14 and 15, respectively. i, Young slique. j, Mature silique. The numbers indicated in the right upper corner represented the flower stages. se, sepal; pe, petal; st, stamen; g, gynoecium. C, Expression of *AtRBM22* gene in response to phytohormones, ABA, IAA and NPA. qRT-PCR were carried out using 10-day-old wild-type seedlings cultured under LDs. Control treatments (Con) were carried out with plants on filter paper saturated with1/2 MS salt solution; ABA (100 μM), IAA (1 μM) and NPA (10 μM) treatments were carried out in 1/2 MS solution for 3h.

3.4.2 Early flowering of *atrbm22* mutants

Salk_132881 (*atrbm22*) carried an insertion in the second exon of *AtRBM22*. It was confirmed as genuine *atrbm22* knockout mutants (Monaghan *et al*., 2010). Full-length genomic AtRBM22 under control of its native promoter complemented the *atrbm22* morphology (Monaghan *et al*., 2010). *atrbm22* mutants were early flowering, and the leaves of *atrbm22* mutants were curled and smaller than WT leaves (Fig. 3-2A,B). These results are consistent with a previous analysis (Monaghan *et al*., 2010). Early flowering phenotype was associated with a reduced leaf number of *atrbm22* mutants (Fig. 3-2C). In addition, *atrbm22* mutants generated shorter siliques (Fig. 3-2D).

A MADS box transcription factor *FLOWERING LOCUS C* (*FLC*) acts as an inhibitor of flowering and functions in the leaf and meristem to delay flowering by repressing floral promoters *FLOWERING LOCUS T* (*FT*) (Samach, *et al*., 2000; Searle *et al*., 2006; Lee *et al*., 2007; Jang *et al*., 2009). *FLC* is a convergence point for several pathways that regulate flowering time in Arabidopsis (Sheldon *et al*., 1999; Michaels *et al*., 2001). In 8-day-old plants, the transcript level of *AtRBM22* was significantly decreased in *atrbm22* mutant (Fig. 3-2E). The expression of *FLC* in *atrbm22* mutants was decreased compared with WT (Fig. 3-2F), while the transcript level of floral promoter *FT* was increased in *atrbm22* mutants (Fig. 3-2G). These results suggest that AtRBM22 plays a role in floral transition in Arabidopsis by regulating the expression of *FLC* and *FT* gene directly or indirectly.

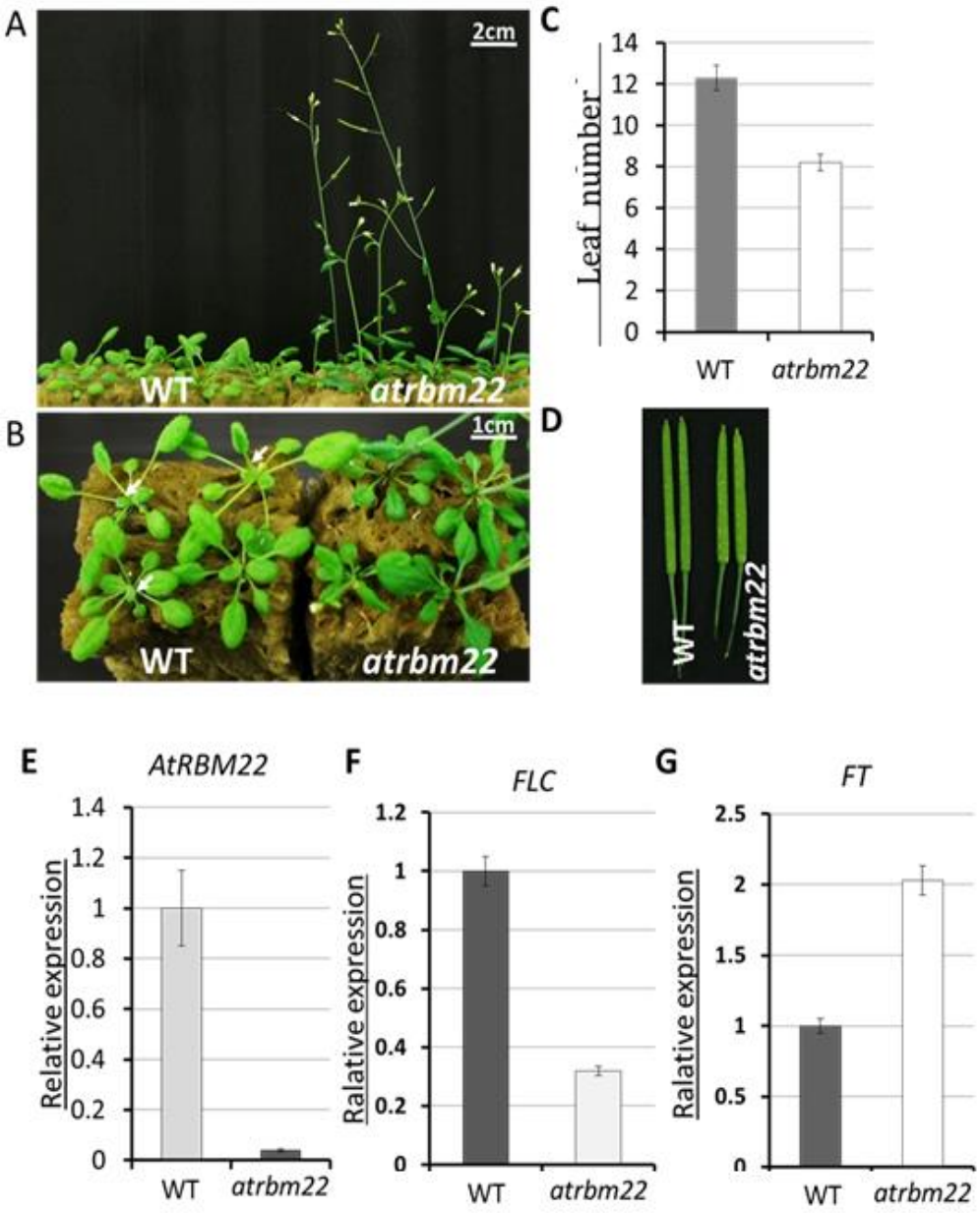

Fig. 3-2. Early flowering of *atrbm22* mutants. A, Photograph illustrating the flowering phenotype of wild-type (WT) plants and *atrbm22* mutants grown under LDs. B, *atrbm22* mutants have twisty leaves indicated by white arrows. C, Numbers of rosette leaves of plants grown under LDs until flowering. D, Shorter silique of *atrbm22* mutants. E-G, qRT-PCR assays. WT plants and *atrbm22* mutants were cultured under LDs for 8 days and then used for qRT-PCR. Values are means ± SE. Experiments were repeated three times.

3.4.3 Overexpression of AtRBM22 leads to repression of inflorescence growth and flower development

Expression of *AtRBM22* was highly restricted in pollen (Fig. 3-1), while the flower of T-DNA knockout mutant was early flowering and produced shorter silique (Fig. 3-2). To get insight into the physiological role of *AtRBM22* gene, the ORF of *AtRBM22* and GFP fusion gene was inserted downstream of the CaMV 35S promoter and used to generate transgenic Arabidopsis plants overexpressing *AtRBM22*. 18 independent overexpressing lines were isolated. In the offspring, an *AtRBM22* overexpressing line (OE2) showed a segregation ratio of 1:2.48 (38:87) for abnormal and normal phenotype. In this line, plants with abnormal phenotype were selected as homozygous plant, abbreviated to OE. AtRBM22:GFP fusion protein was observed in the nucleus in the transgenic plants (Fig. 3-3A). The transcript level of *AtRBM22* in homozygous plants was higher than wild type plants (Fig. 3-3B).

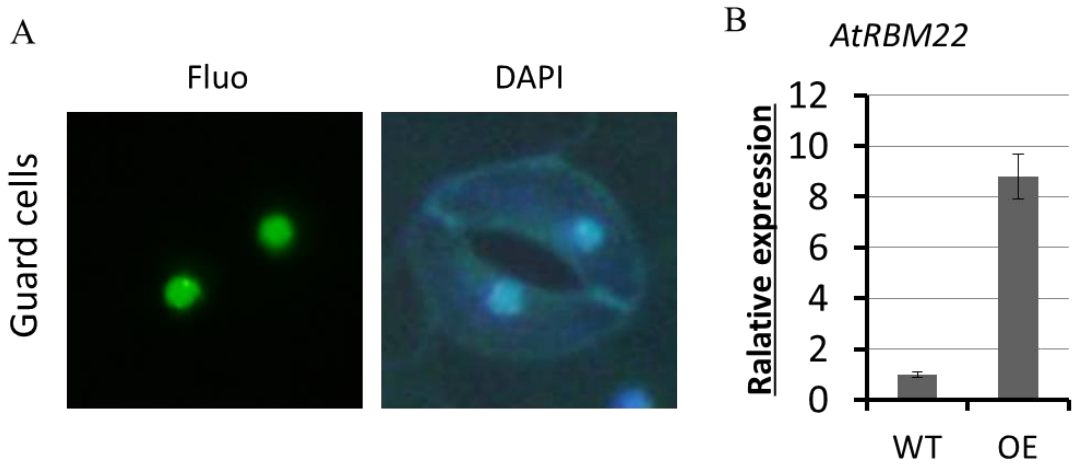

Fig. 3-3. Plant overexpressing AtRBM22:GFP fusion gene. A, AtRBM22:GFP fusion protein was located in the nuclei of guard cells. Fluo: fluorescence from GFP. To visualize the nucleus, plant leaves were stained by 4',6-diamidino-2-phenylindole (DAPI). B, qRT-PCR. Total RNA for qRT-PCR analysis was isolated from leaves of WT (Col-0) and homozygous plants (OE).

The phenotype of the inflorescence, flower and silique of OE plants were obviously different from these of control plants (Con) overexpressing GFP alone (Fig. 3-4). Compact inflorescence resulted from the shorter peduncle of OE plants (Fig. 3-4A). Floral organs including petal, stamen and carpel of OE plants were shorter than these of control plants, while the sepal of OE plants was similar with that of control plants in size (Fig. 3-4B,F,G). Even more serious phenotype observed from OE plants was that the petal, stamen and carpel were withered in a great mount of flowers (Fig. 3-4H). The siliques of OE plants were approximately 50% shorter than that from control plants (Fig. 3-4E). Most of the embryos failed to develop into mature seeds in OE plants (Fig. 3-4I). Similar phenotypes of inflorescence and silique were observed from almost all the independent transgenic lines examined (Fig. 3-4G,K). The vegetative growth of the transgenic plants was normal (Fig. 3-4 L). These results suggest that AtRBM22 is critical for the floral organ development of Arabidopsis.

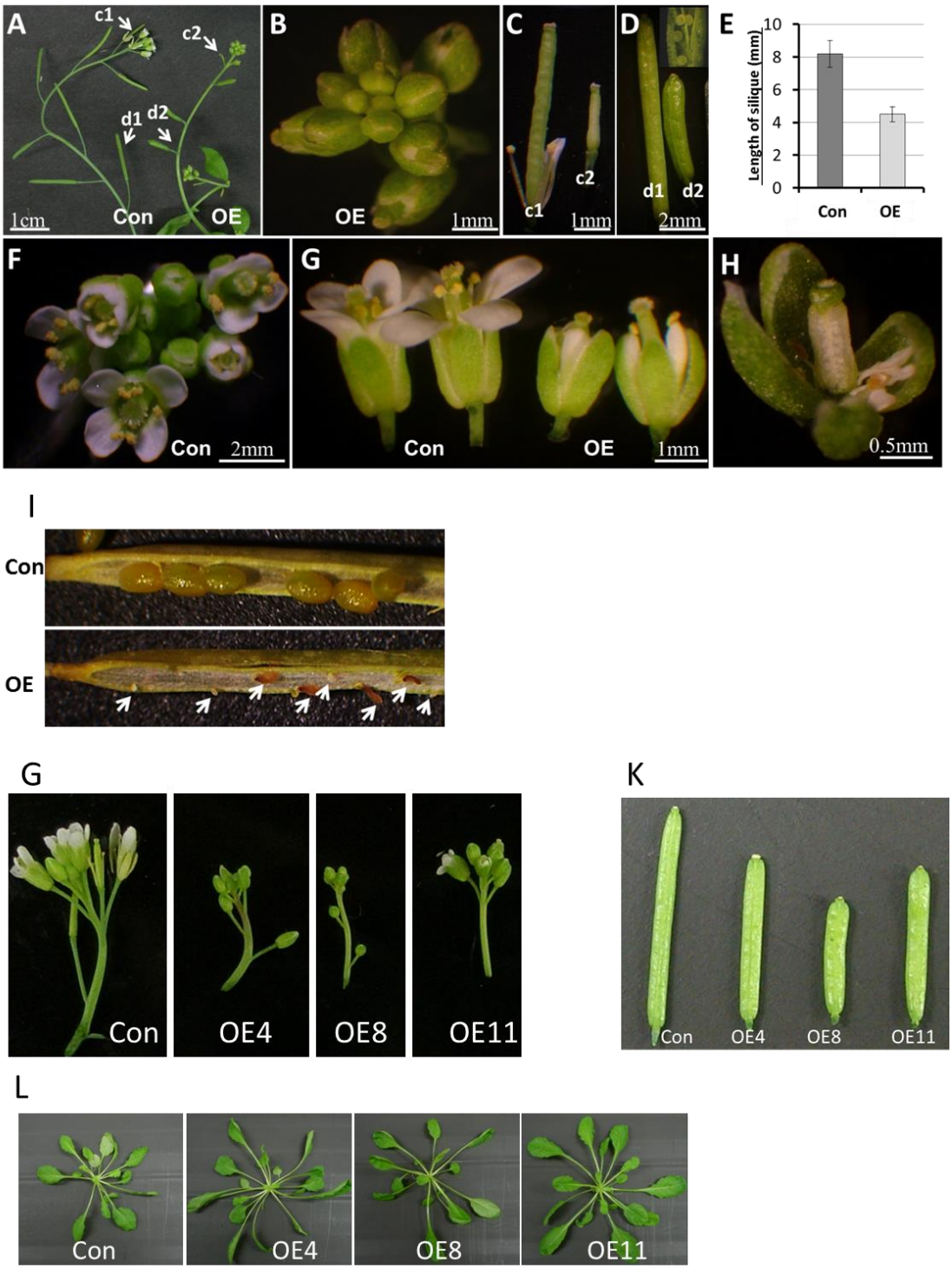

Fig. 3-4. The phenotypes of homozygous plants (OE). A comparison of the inflorescence of plant overexpressing GFP alone (Con) and OE plants grown under SDs. B and F, Enlarged views shown the apexes of Con and OE plants. G, Detached flowers showing the shorter petal, stamen and carpel of OE flowers. C and D, Enlarged views shown the siliques indicated by c1, c2, d1 and d2 in panel A. View of embryos of OE plants was enlarged in the right top. E, Silique length in

Con and OE plants. Values are means ± SE. H, The petal, stamen and carpel of a great mount of flowers were withered in OE plants. I, Most of the embryos failed to develop into mature seeds in OE plants. White arrows indicated the embryos of OE plants. G-L, Phenotypes of other homozygous lines cultured under SDs. OE4, OE8 and OE11 represented independent transgenic lines.

A significantly dwarf phenotype was observed from homozygous plants (Fig. 3-5A). Auxin constitutes a class of phytohormones which control the apical dominance and affect several distinct processes needed for full development of fecundity in Arabidopsis. Therefore, the expression of auxin-responsive genes in mature OE plants was examined (Fig. 3-5B). Compared with WT, transcriptions of early auxin-regulated genes *GH3.3*, *SAUR9*, *IAA5* were slightly increased in OE plants, while transcription of *IAA19* was decreased. A homeobox-leucine zipper protein HAT2 took part in auxin mediated signaling pathway and negative regulation of transcription. The transcript level of HAT2 was medially upregulated in OE plants. *LATERAL ORGAN BOUNDARIES DOMAIN 29* (*LBD29*), an important molecule downstream of auxin response factors, was significantly upregulated in OE plants. On the other hand, the expression of other auxin-responsive genes (*CH3.4*, *SAUR15*, *SAUR66*, *IAA1* and *IAA6*) were not affected in OE plants (data not shown). These results indicate that AtRBM22 plays a role in controlling the expression of specific auxin-responsive genes, and the dwarf phenotype of OE plants result from the changed expression of some auxin-responsive genes.

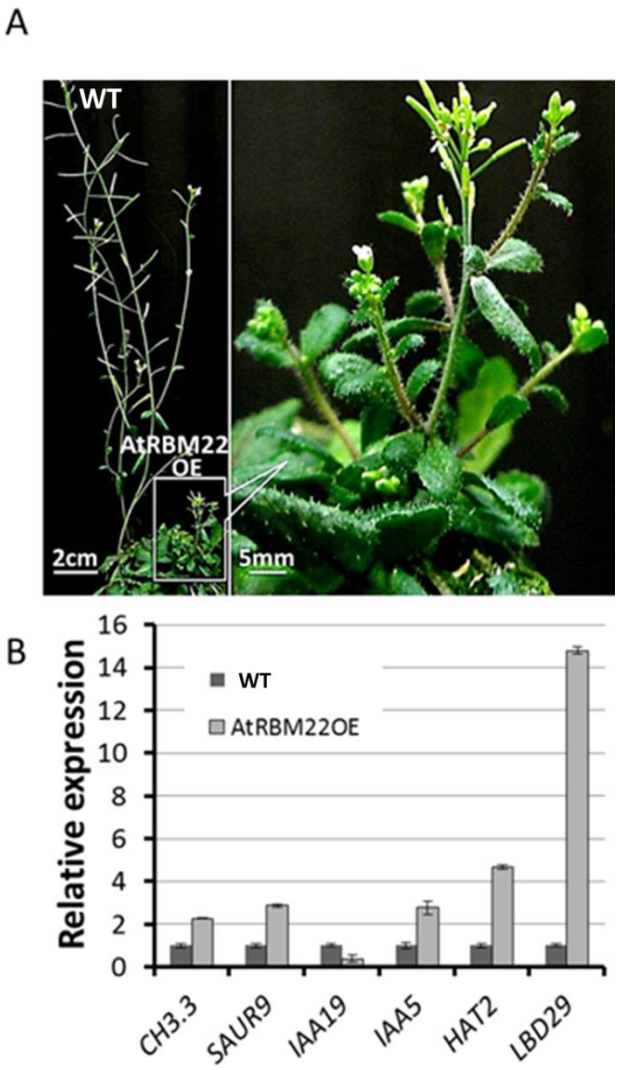

Fig. 3-5. A, The dwarf phenotype of mature homozygous plant (AtRBM22OE) grown under SDs. View of OE plant shown in the left panel was enlarged in the right panel. B, qRT-PCR analysis of expression of auxin-responsive genes in OE plants. Total RNA for qRT-PCR analysis was isolated from flowering plants. Actin was used as an internal control. Values were means ± SE. Experiments were repeated three times.

3.4.4 AtRBM22 is involved in ABA response

The expression of AtRBM22 was slightly induced by ABA (Fig. 3-1C), which was consistent with publicly available microarray data (Kilian *et al*., 2007). A well-established function of ABA is to promote seed dormancy and to inhibit seed germination (Christmann *et al*., 2006). In the absence of exogenous ABA, OE and *atrbm22* mutant seeds germinated as well as wild type Col-0 seeds (WT, Fig. 3-6A, left panel). In the presence of 1 μM ABA, the germination of OE and *atrbm22* seeds was earlier than that of WT seeds (Fig. 3-6A, right panel). After germination, the greening rates of OE plants and *atrbm22* mutants were higher than that of WT (Fig. 3-6B). The primary roots of OE plants and *atrbm22* mutants were longer than WT (Fig. 3-6C,D).

3.4.5 Plants overexpressing AtRBM22 are sensitive to NaCl

Salt stress and ABA signaling pathways constitute a complex network (Xiong *et al*., 1999). The NaCl sensitivity at seed germination stage was also determined. OE and *atrbm22* seeds germinated as well as WT seeds on the medium without NaCl (Fig. 3-7, left panel). Either in the presence of 100 or 150 mM NaCl, the germination of OE seeds was late (Fig. 3-7A, middle and right panel, respectively). To get insight into whether OE plants were sensitive to NaCl, WT, OE and *atrbm22* seedlings were cultured for three days on medium without any treatment, and then transferred onto medium with NaCl (200 mM) or without NaCl. As a result, OE seedlings were more sensitive than WT and *atrbm22* mutants (Fig. 3-7C upper panel).

These data suggest that AtRBM22 plays roles in stress response. Genetic and molecular studies have suggested that there is extensive interaction between salt stress and ABA responses. Both positive and negative interactions depended on the nature

and duration of the treatments (Xiong *et al.*, 1999). The different responses of OE plants and *atrbm22* mutants may be related to the treatments. The role of AtRBM22 in stress response should be studied in future.

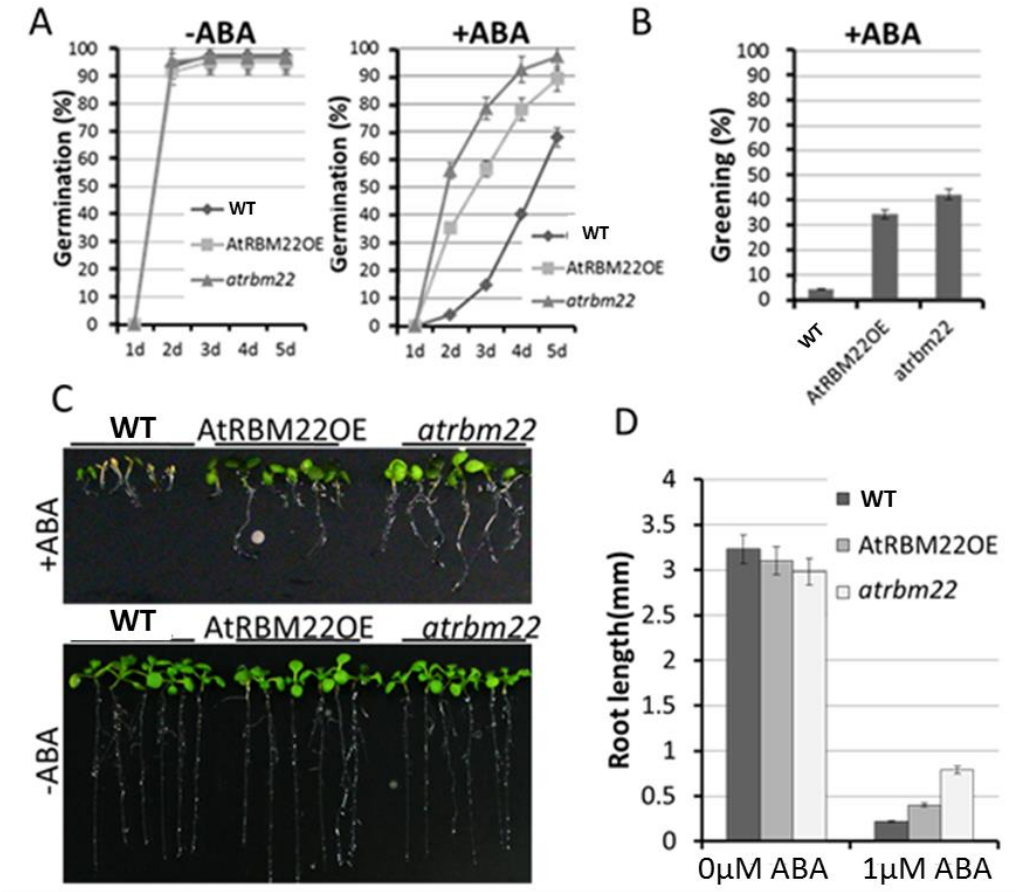

Fig. 3-6. Constitutive expression of AtRBM22 and AtRBM22 mutation result in ABA insensitivity of plants. A, The germination rates of WT, AtRBM22OE and *atrbm22* mutant seeds sowed on ½ MS medium with 1 μM ABA (right panel) or without ABA (left panel). 50 seeds of each line were examined. B, The greening rates of seedlings grown on ½ MS medium with ABA for 8 days. C, Views of seedlings grown on ½ MS medium with 1 μM ABA (upper panel) without ABA (lower panel) for 8 days. D, Root length of 8-d-old seedlings grown on ½ MS medium with or without ABA. Values are means ± SE. Experiments were performed in triplicate.

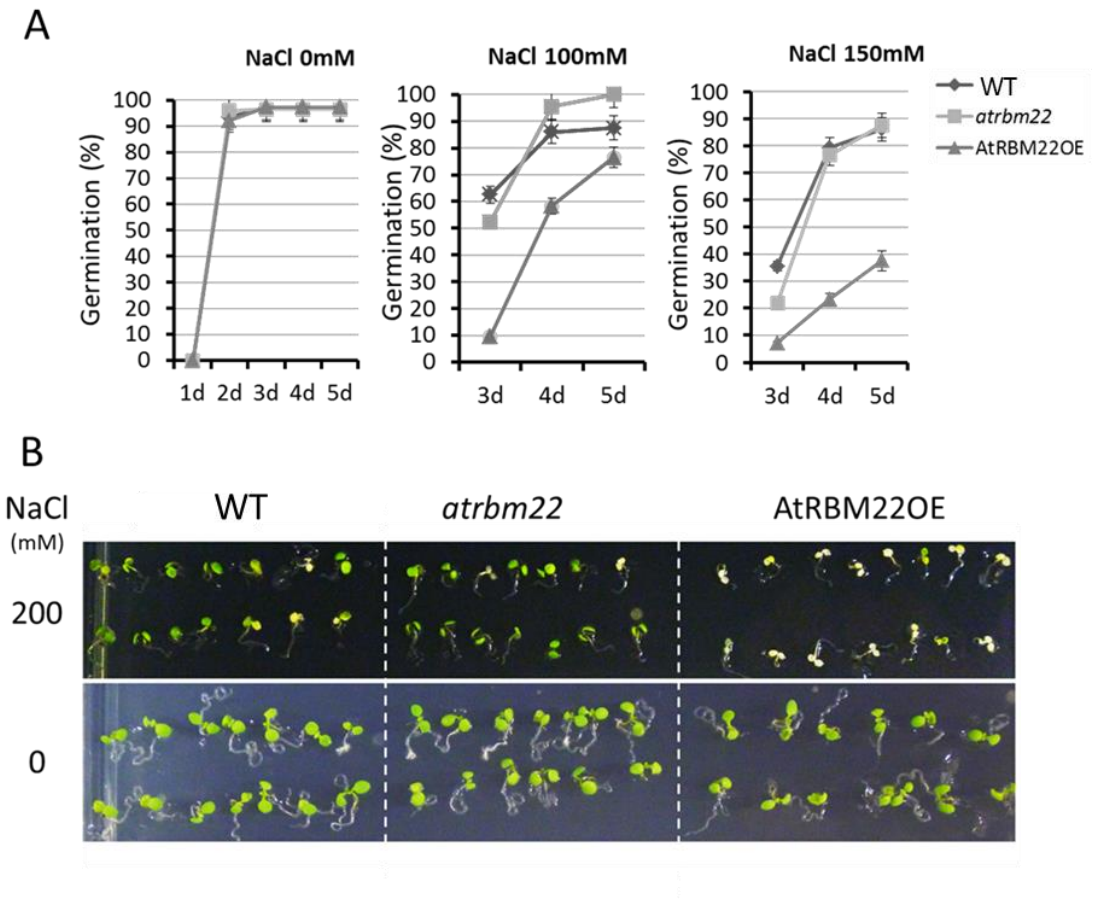

Fig. 3-7. Constitutive expression of AtRBM22 results in salt sensitivity of plants. A, The germination rates of WT, OE and *atrbm22* mutant seeds exposed to 0, 100 and 150 mM NaCl. 50 seeds of each line were used. Values are means ± SE. B, Views of 3-d-old seedlings were grown on ½ MS medium and subsequently transferred onto ½ MS medium containing NaCl (200 mM) for additional 5 days. Experiments were performed in triplicate.

3.5 Discussion

AtRBM22 was predominantly expressed in in pollen in the third whorl (Fig. 3-1). Floral organs including petal, stamen and carpel of OE plants were shorter than these of Con plants (Fig. 3-4). In contrast, the sepals of OE plants were as long as that of Con plants. Meanwhile, short siliques and reduced seed production was found in the AtRBM22 overexpressing plants. These results suggest that AtRBM22 plays roles in the development of petal, stamen and carpel in Arabidopsis.

In Arabidopsis, Four major classes of homeotic genes, A, B, C and E, confer the four floral organs in a combinatorial manner (reviewed in Krizek and Fletcher, 2005). The class A genes confer sepal identity in the first whorl. Petal identity is specified in the second whorl by the class A genes and the class B genes. Stamen identity is determined in the third whorl by the combined activity of the class B genes and the class C genes. Carpel identity is conferred by the class C genes in the fourth whorl. Class E genes are required for the identification of all of these four organs. In Arabidopsis, *HUA1*, encoding an RNA binding protein with six CCC-type zinc fingers, acts in the floral morphogenesis by specifically promoting the processing of a class C gene *AGAMOUS* (*AG*) pre-mRNA (Li *et al*., 2001; Cheng *et al*., 2003). RABBIT EARS (RBE), which acts downstream of a class A gene, *APETALA1* (*AP1*), and is a repressor of *AG* misexpression in the second whorl (Takeda *et al*., 2003; Krizek, *et al*, 2006), was identified as an AtRBM22-interacting protein (Fig. 2-5). These results indicate that *AtRBM22* functions in combination with the class B, C and E genes to regulate the development of petal, stamen and carpel.

The flowering time was determined in the early stage of plant vegetative development (Fornara *et al*., 2010). The transcript levels of AtRBM22 gene was relative lower in young seedlings. In Arabidopsis, AtRBM22 and F16P2.4 double mutant is lethal (Monaghan *et al*., 2010). AtRBM22 and F16P2.4 are unequally redundant, and AtRBM22 is the dominant contributor of the pair (Monaghan *et al*.,

2010). AtRBM22 deficiency caused early flowering (Fig. 3-2), indicating that *AtRBM22* play a role in the floral transition in the early stage of plant development. In conclusion, AtRBM22 is required for the development of Arabidopsis.

Chapter 4

A type-2C protein phosphatase (AtPP2C52) interacts with heterotrimeric G protein beta subunit in Arabidopsis

4.1 Abstract

Protein dephosphorylation plays multiple roles in regulating nearly every aspect of cell life. In this research, a type-2C protein phosphatase, AtPP2C52, was localized in the plasma membrane and a mutation in the putative myristoylation site of AtPP2C52 disrupted its plasma membrane localization. AtPP2C52 promoter-GUS analysis revealed that *AtPP2C52* gene was found in a broad expression pattern with a higher level in the vascular and meristem. AtPP2C52 was identified as a target of Arabidopsis G protein β subunit (AGB1). AtPP2C52 can interact with the other proteins, including a proteasome maturation factor, UMP1, and a cysteine proteinase, RD21a. By mutational analysis of AtPP2C52, it was identified that some residues were essential for AtPP2C52 to bind AGB1, UMP1 and RD21a, suggesting that these residues are critical for the function of AtPP2C52.

4.2 Introduction

Protein phosphorylation regulates almost all aspect of cell life (Hunter, 1998; Cohen, 1997). In the process of protein phosphorylation, protein kinases are in charge of adding one or more phosphate groups to certain amino acid residues of their target proteins, while protein phosphatases are in charge of removing these phosphate groups. In Arabidopsis genome, 112 protein phosphatases have been identified (Kerk *et al*., 2002). Protein phosphatases have been considered to be much more flexible enzymes, which have a larger number of substrates and present with overlapping activities (Lammers and Lavi, 2007).

Based on the substrate specificity and on the conservation of the catalytic domain, protein phosphatases were grouped into protein serine/threonine (Ser/Thr) phosphatases and protein tyrosine phosphatases. Protein Ser/Thr phosphatases were classified into phosphoprotein phosphatases (PPPs) and metal-dependent protein phophatases (PPMs). The PPM family contains type-2C protein phosphatase (PP2C) subfamily and pyruvate dehydrogenase phosphatase (Cohen, 1997).

PP2Cs were found in all organisms, such as plants, bacteria, yeast, nematodes, insects, and mammals (Schweighofer *et al*., 2004). A distinguishing feature of PP2Cs is the requirement of bivalent cation (Mn^{2+} or Mg^{2+}) for their catalytic activity. Meanwhile, the intracellular concentrations of Mg^{2+} and Mn^{2+} do not fluctuate substantially under physiological conditions. Therefore, the activities of PP2Cs may be controlled predominantly by their tissue- or cell type-specific expression, subcellular compartmentalization, post-translational modification, or/and degradation (Lammers and Lavi, 2007).

In Arabidopsis, seventy-six PP2C genes were identified (Kerk *et al*., 2002). These genes were clustered into several groups, based on their sequence similarity

(Schweighofer *et al*., 2004; Xue *et al*., 2008). Group A PP2C genes are annotated as negative regulators of the ABA response in plant (Hirayama and Shinozaki, 2007). On the other hand, SNF1-related protein kinase 2 (SnRK2) family, which is activated by ABA or osmotic stress, positively regulates the ABA response in various tissues (Mustilli *et al*., 2002; Yoshida *et al*., 2002; Fujii *et al*., 2007). Group A PP2Cs interacted physically with SnRK2s in various combinations, and efficiently inactivated SnRK2s via dephosphorylation of multiple Ser/Thr residues in the activation loop (Umezawa *et al*., 2009). In response to ABA, PP2C-dependent negative regulation can be canceled by ABA receptors, RCAR/PYRs, leading to activation of positive regulatory pathways (Ma *et al*., 2009; Park *et al*., 2009). Group A PP2Cs interacted physically with RCAR/PYRs. Members of Group B PP2C were shown to regulate stomata aperture, seed germination, abscisic acid inducible gene expression, and interact and inactivate mitogen-activated protein kinase (MAPK, Umbrasaite *et al*., 2010).

AtPP2C52 was clustered into Group E (Xue *et al*., 2008). In this study, the interaction between the heterotrimeric G proteins β subunit (AGB1) and AtPP2C52 has been confirmed by Y2H analysis and an *in vitro* Co-IP assay. *AtPP2C52* is expressed in almost all the plant organs with a higher level in the vascular and meristem. AtPP2C52 can interact with UMP1 and RD21a as well as AGB1.

4.3 Materials and methods

4.3.1 Plant materials and growth conditions

Arabidopsis Col-0 plants were used. Seeds were surface sterilized in 70% (v/v) ethanol solution for 30sec, then sterilized in 0.25% (v/v) sodium hypochlorite containing 1% (v/v) Tween X-100 and washed four times in sterile distilled water. Afterward, seeds were sowed on MS plates containing half MS basal salts (Wako) and 1% (w/v) sucrose, pH 5.7, solidified with 0.8% (w/v) agar (Wako). Plates were sealed and incubated in 4℃ for 72h in darkness, then transferred to growth chamber incubated at 22℃. Light intensity is 120 μmol m^{-2} s^{-1}. After ten days of growth, plants were transferred onto rockwool cubes and grown further with 0.2×MS solution regularly supplied.

4.3.2 Yeast two-hybrid (Y2H) assay

Full-length cDNA clone of *AGG1* (*AT3G63420*) and *AtPP2C52* (*AT4G03415*) (RAFL22-41-E11 and RAFL18-04-O14, respectively) were obtained from RIKEN BRC Experimental Plant Division (Seki *et al.*, 2002). The ORF of *AGG1* was amplified by PCR using the cDNA cloned as template and the following primer pair: 5’-GGGCATATGCGAGAGGAAACTGTGG-3’ and 5’-CCACTAGTAAGTATTAAGCATCTGCAGCC-3’ (*Nde*I and *Spe*I sites are underlined). The PCR products were digested by *Nde*I and *Spe*I, and cloned into the *Nde*I-*Xba*I site of pGADT7-rec, generating pGAD-AGG1. The open reading frame (ORF) of *AtPP2C52* was amplified by PCR using the cDNA clone as template and the following primer pair: 5’-CCCGAATTCTCTAGAATGGGGGGTTGTGTGTCGAC-3’ (*Eco*RI and *Xba*I sites are underlined) and 5’-GGGCTCGAGGAGTCTTCGATTTCTCTTCAGAG-3’

(*Xho*I site is underlined). The PCR products were digested by *Eco*RI and *Xho*I, and cloned into the *Eco*RI/*Xho*I site of pGADT7-rec, generating pGAD-*AtPP2C52*. The ORF of *AtPP2C1* (*AT1G03590*) was amplified by reverse transcription-PCR (RT-PCR) using cDNA synthesized from total RNA from 2-week-old Arabidopsis seedlings as template and the following primer pair: 5'-GGGCATATGGGAGGTTGTATCTCTAAG-3' and 5'-GAGGTCGACAAGTCTTTGGTTCCTCTCCAGGG-3' (*Nde*I and *Sal*I sites are underlined). The PCR products were digested by *Nde*I and *Sal*I, and cloned into the *Nde*I-*Xho*I site of pGADT7-rec, generating pGAD-AtPP2C1. The ORF of *AtPP2C74* (*AT5G36250*) was amplified by RT-PCR using the following primer pair: 5'-CGCCATATGGGGTCCTGCTTATCATC-3' and 5'-CCCGTCGACACTCTTTGGTTGGGACATATAC-3' (*Nde*I and *Sal*I sites are underlined). The PCR products were digested by *Nde*I and *Sal*I, and cloned into the *Nde*I-*Xho*I site of pGADT7-rec, generating pGAD-AtPP2C74.

The point mutations of *AtPP2C52* gene were generated by PCR using PrimeSTAR (TaKaRa) with wild type *AtPP2C52* cDNA as template. For the point mutation of *AtPP2C52*^{G99D}, PCR was performed using the following primer pair: G99D-Fw 5'-GTGACATTTTGTGATGTATTTGATGGTCATGGTCC-3' and *AtPP2C52*-Rv 5'-GAGTCGGATCCTCAAGTCTTCGATTTCTCTTC-3' (*Bam*HI site is underlined), generating 3'- terminus of *AtPP2C52*^{G99D}. To generate 5'- terminus of *AtPP2C52*^{G99D}, PCR was performed using the following primer pair: *AtPP2C52*-Fw 5'-GAGTCGAATTCATGGGGGGTTGTGTGTC-3' (*Eco*RI site is underlined) and G99D-Rv 5'-GACCATCAAATACACCACAAAATGTCACATCTTCAGAC-3'. Subsequently, the mixture of 3'- and 5'-terminus of *AtPP2C52*^{G99D} was used as template for PCR using primer pair *AtPP2C52*-Fw and *AtPP2C52*-Rv, generating full-length *AtPP2C52*^{G99D}. The PCR products of *AtPP2C52*^{G99D} were digested by *Eco*RI and *Bam*HI, and cloned into the *Eco*RI/*Bam*HI site of pGADT7-rec, generating pGAD-*AtPP2C52*^{G99D}. For the point mutation of *AtPP2C52*^{G105D}, PCR was performed

using the following primer pair: G105D-Fw 5’-GATGGTCATGATCCTTATGGCCATCTTGTTGCTCG-3’ and *AtPP2C52*-Rv, generating 3’-terminus of *AtPP2C52*^{G105D}. To generate 5’-terminus of *AtPP2C52*^{G105D}, PCR was performed using the following primer pair: *AtPP2C52*-Fw and G105D-Rv 5’-GCCATAAGGATCATGACCATCAAATACACCACAAAATG-3’. Subsequently, the mixture of 3’- and 5’-terminus of *AtPP2C52*^{G105D} was used as template for PCR using primer pair *AtPP2C52*-Fw and *AtPP2C52*-Rv, generating full-length *AtPP2C52*^{G105D}. The PCR products of *AtPP2C52*^{G105D} were digested by *Eco*RI and *Bam*HI, and cloned into the *Eco*RI/*Bam*HI site of pGADT7-rec, generating pGAD-*AtPP2C52*^{G105D}. For the point mutation of *AtPP2C52*$^{DGH102-104ERN}$, PCR was performed using the following primer pair: DGH102-104ERN-Fw 5’-GGTGTATTTGAACGTAATGGTCCTTATGGCCATCTTG-3’ and *AtPP2C52*-Rv, generating 3’-terminus of *AtPP2C52*$^{DGH102-104ERN}$. To generate 5’-terminus of *AtPP2C52*$^{DGH102-104ERN}$, PCR was performed using the following primer pair: *AtPP2C52*-Fw and DGH102-104ERN-Rv 5’-CATAAGGACCATTACGTTCAAATACACCACAAAATGGC-3’. Subsequently, the mixture of 3’- and 5’-terminus of *AtPP2C52* $^{DGH102-104ERN}$ was used as template for PCR using primer pair *AtPP2C52*-Fw and *AtPP2C52*-Rv, generating full-length *AtPP2C52*$^{DGH102-104ERN}$. The PCR products of *AtPP2C52* $^{DGH102-104ERN}$ were digested by *Eco*RI and *Bam*HI, and cloned into the *Eco*RI/*Bam*HI site of pGADT7-rec, generating pGAD-*AtPP2C52*$^{DGH102-104ERN}$. These mutations were confirmed by sequencing and then used for yeast transformation.

Full-length cDNA of *UMP1* (AT1G67250) and *RD21a* (AT1G47128) were ordered from ABRC and used as PCR templates for following plasmids construction. The ORF of *UMP1* was amplified by PCR using the cDNA clone as template and the following primer pair: 5’-GAGTCGAATTCATGGAGTCTGAGAAAAAGATAGCTCATG-3’ (*Eco*RI site is underlined) and 5’-GAGTCGGATCCTTACATGAAACTTGGGTAAATCGG-3’

(*Bam*HI site is underlined). The PCR products were digested by *Eco*RI and *Bam*HI, and cloned into the *Eco*RI/*Bam*HI site of pGADT7-rec, generating pGAD-*UMP1*. The ORF of *RD21a* was amplified by PCR using the cDNA clone as template and the following primer pair: 5'-GAGTCGAATTCATGGGGTTCCTTAAGCCAACCATGGC -3' (*Eco*RI site is underlined) and 5'-GAGTCCCTAGGTTAGGCAATGTTCTTTCTGCCTTGTGACCAG-3' (*Bam*HI site is underlined). The PCR products were digested by *Eco*RI and *Bam*HI, and cloned into the *Eco*RI/*Bam*HI site of pGADT7-rec, generating pGAD-*RD21a*.

Yeast transformation using yeast strain AH109 and screening were performed by Matchmaker Gold Yeast Two-Hybrid System (Clontech). At least 5 colonies grown on the SD media lacking leucine and tryptophan (SD/-Leu/-Trp), were streaked on the SD/-Leu/-Trp and the SD media lacking leucine, tryptophan, adenine, and histidine (SD/-Trp/-Leu/-His/-Ade). Photos were taken after the yeasts were cultured for 3-5 days. The experiments were performed for three times.

4.3.3 *In vitro* pull-down assay

For the *in vitro* pull-down assay, pGAD-AtPP2C52 was digested by *Eco*RI and *Xho*I, and the resultant ORF fragments of *AtPP2C52* were inserted into the *Eco*RI-*Xho*I site of pGEX-5X-1 (GE Healthcare) in-frame to the coding sequence of glutathione S-transferase (GST), generating pGEX-5X-AtPP2C52. The coding sequence of *Myc*-tagged *AGB1* was amplified using pGBK-AGB1 as template and the following primer pair: 5'-CCCTCTAGAAATAATTTTGTTTAACTTTAAGAAGGAGATATACATATGGAG GAGCAGAAGCTGATC-3' and 5'-CCCGTCGACAATCACTCTCCTGGTCCTCC-3' (*Xba*I and *Sal*I sites are underlined). The PCR products were digested by *Xba*I and *Sal*I, and inserted into the *Xba*I-*Sal*I site of pET32b(+) (Novagen), generating

pET-Myc-AGB1. To induce GST-fused AtPP2C52 (GST-AtPP2C52) and Myc-tagged AGB1, pGEX-5X-AtPP2C52 and pET-Myc-AGB1 were transformed into the *E. coli* strain, BL21 (DE3). Transformed *E. coli* cells were cultured at 37 °C in LB medium until OD_{600} reached 0.5, and incubated at 28 °C for 2 h after addition of IPTG to a final concentration of 0.2 mM. The cells were then harvested by centrifugation and resuspended in 1× TBS (Tris-buffered saline: 150 mM NaCl in 20 mM Tris-HCl, pH 7.5) with 2 mg/ml lysozyme (Wako, Japan). The cell suspension was frozen at -80 °C and thawed at room temperature. Freezing and thawing were repeated two more times to lyse the cells, and 2 units of recombinant DNase I (Takara Bio) was added to the solution. The solution was incubated at room temperature until the solution became fluid due to DNA degradation. The solution was then centrifuged at 12000 × g for 5 min and the supernatant was used as crude protein extracts.

GST-AtPP2C52 in the crude extracts was bound to Glutathione Sepharose 4 Fast Flow (GE Healthcare) following the manufacturer's instructions and the resin was washed 4 times by 1× TBS. After removing 1× TBS, the resin was resuspended in the crude extracts containing Myc-AGB1 and incubated at room temperature for 60 min with gentle shaking. The resin was then washed 4 times by 1× TBS and resuspended in 20 mM reduced glutathione in 50 mM Tris-HCl, pH 8.0. The suspension was incubated at room temperature for 15 min to elute GST-AtPP2C52. The slurry of the resin was centrifuged for a few min at 12000 × g, and GST-AtPP2C52 and Myc-AGB1 in the supernatant were analyzed by immunoblotting using an anti-GST antibody (GE Healthcare) and an anti-Myc antibody (Medical & Biological Laboratories Co. Ltd. (MBL), Japan). To detect signals of Myc-AGB1 in the GST pull-down assay, SuperSignal West Femto Chemiluminescent Substrate (Thermo Fisher Scientific) was used. For the other immunoblot experiments, SuperSignal West Pico Chemiluminescent Substrate (Thermo Fisher Scientific) was used.

4.3.4 Western blotting

Proteins were expressed by TNT Quick Coupled Transcription/Translation Systems (Promega). Plasmid DNA pGAD-*AtPP2C52*, pGAD-*AtPP2C52*^{G99D}, pGAD-*AtPP2C52*^{G105D}, pGAD-*AtPP2C52* $^{DGH102-104ERN}$ and pGADT7-rec vector were used to synthesize proteins, respectively. Co-IP was carried out using anti-HA antibody **(**MBL) following the MATCHMAKER Co-IP Kit User Manual (Cat No. 630449, 2003).

4.3.5 Bimolecular Fluorescence Complementation (BiFC) assay

The vectors for BiFC assay were constructed by replacing GFP in the vector pBS-35SMCS:GFP (Tsugama *et al*., 2012) with the N-terminus (154 amino acids) or the C-terminus (80 amino acids) of YFP, generating pBS-35SMCS-nYFP and pBS-35SMCS-cYFP, respectively. The pGAD-AtPP2C52 was digested by *Xba*I and *Xho*I, and the resultant ORF fragments of *AtPP2C52* were inserted into the *Xba*I/*Sal*I site of pBS-35SMCS-cYFP, generating pBS-35S-AtPP2C52-cYFP. The ORF of *UMP1* without stop codon was amplified by PCR using the cDNA clone as template and the following primer pair: 5'-GAGTCGGTACCATGGGGTTCCTTAAGCCAAC-3' (*Kpn*I site is underlined) and 5'-CTCGAACTAGTGGCAATGTTCTTTCTGC-3' (*Spe*I site is underlined). The PCR products were digested by *Kpn*I and *Spe*I, and cloned into the *Kpn*I/*Spe*I site of pBS-35SMCS-nYFP, generating pBS-35S-nYFP-*UMP1*. The ORF of *RD21a* without stop codon was amplified by PCR using the cDNA clone as template and the following primer pair: 5'-GAGTCGGTACCATGGAGTCTGAGAAAAAGATAGC-3' (*Kpn*I site is underlined) and 5'-CTCGAACTAGTCATGAAACTTGGGTAAATCGG-3' (*Spe*I site is underlined). The PCR products were digested by *Kpn*I and *Spe*I, and cloned into the *Kpn*I/*Spe*I site of pBS-35SMCS-nYFP, generating pBS-35S-nYFP-*RD21a*. Arabidopsis protoplast

isolation and transformation were conducted as described (Wu *et al*., 2009). Plasmids DNA were introduced into onion epidermal cells by a bombardment system (Bio Red, PDS-1000). Images were processed using Canvas X software (ACD Systems) and enhanced using Photoshop CS4 software (Adobe).

4.3.6 Preparation of chimeric constructs

An approximately 2kb upstream promoter sequence of *AtPP2C52* ($P_{AtPP2C52}$) was cloned from an Arabidopsis cDNA by using primer pair: 5'-GGATCCCGGGATGAATCATGTAGGTGAC-3' (*Sma*I site is underlined) and 5'-CCCTCTAGATGTTTAATCCCAGCCTAGA-3' (*Xba*I site is underlined). The PCR products were double-digested with *Sma*I/*Xba*I and used to replace the CaMV 35S promoter of pBI121 vector (Clontech, Bevan, 1984), generating pBI121-$P_{AtPP2C52}$::*GUS*. pGAD-*AtPP2C52* was digested by *Xba*I and *Xho*I, and the resultant ORF fragments of *AtPP2C52* were inserted into the *Xba*I/*Sal*I site of pBS-35SMCS:GFP, generating pBS-35S::*AtPP2C52:GFP*. To introduce the glycine $\rightarrow$ alanine mutation at position 2 (G2A mutation) of PP2C52, the ORF of *PP2C52* was amplified by PCR using pBS-35S-PP2C52:GFP as template and the following primer pair: 5'-GGGTCTAGAATGGCGGGTTGTGTGTCGACTAGTAG-3' and 5'-GGGCTCGAGGAGTCTTCGATTTCTCTTCAGAG-3' (*Xba*I and *Xho*I sites are underlined). The PCR products were digested by *Xba*I and *Xho*I, and inserted into the *Xba*I-*Xho*I site of pBS-35SMCS:GFP. The pBS-35S::*AtPP2C52:GFP* plasmid was were double-digested with *Xba*I/*Sac*I site and inserted to pBI121 vector, generating pBI121-35S::*AtPP2C52:GFP*.

4.3.7 Plant transformation

Arabidopsis Col-0 plants were transformed by *Agrobacterium tumefaciens*-mediated transformation using the floral-dip method (Clough and Bent,

1998). The *Agrobacterium* strain used was EHA105 harboring binary vector pBI121 carrying the 35S::*AtPP2C52:GFP* or $P_{AtPP2C52}$::*GUS* fusion gene.

4.3.8 GUS histochemical analysis

For GUS histochemical characterization of the $P_{AtPP2C52}$::GUS lines, several developmental stages were examined. Samples were treated with 90% acetone for 30 min at 4℃, immersed in a staining solution (5 mM X-gluc, 0.1% Triton X-100, 0.5 mM $K_3Fe(CN)_6$, 0.5 mM $K_4Fe(CN)_6$, 10 mM Na_2EDTA and 50 mM sodium phosphate buffer, pH7.0), vacuum infiltrated for more than 1 hour, then incubated at 37℃ for 24 h. After staining, samples were cleared by several changes of 70% ethanol. Photographs were enhanced using Photoshop CS4 software (Adobe).

4.3.9 Phosphatase assay

GST-AtPP2C52 was expressed in *E. coli* and bound to Glutathione Sepharose 4 Fast Flow as described above. The resin was washed 4 times by 1× TBS and resuspended in 20 mM reduced glutathione in 50 mM Tris–HCl, pH 8.0. To elute GST-AtPP2C52. The slurry was centrifuged at 6000 ×g for 2 min and the supernatant was used as purified GST-AtPP2C52 solution for the phosphatase assay. To express polyhistidine-tagged AGB1 (His-AGB1), the ORF of AGB1 was amplified by PCR using pGBK-AGB1 as template and the following primer pair: 5′-CGCTCTAGAATGTCTGTCTCCGAGCTC-3′ and 5′-CCCGTCGACAATCACTCTCCTGGTCCTCC-3′ (*Xba*I and *Sal*I sites are underlined). The PCR products were digested by *Xba*I and *Sal*I, and cloned into the *Nhe*I-*Xho*I site of pRSETB (Invitrogen), generating pRSET-AGB1. To express polyhistidine-tagged AGG1 (His-AGG1), the ORF of AGG1 was amplified by PCR using the cDNA cloned as template and the following primer pair: 5′-GGGTCTAGAATGCGAGAGGAAACTGTGG-3′ and

5′-CCGTCGACAAGTATTAAGCATCTGCAGCC-3′ (*Xba*I and *Sal*I sites are underlined). The PCR products were digested by *Xba*I and *Sal*I, and cloned into the *Nhe*I-*Xho*I site of pRSETB, generating pRSET-AGG1. pRSET-AGB1 or pRSET-AGG1 was introduced into BL21 (DE3). Transformed cells were cultured overnight at 37 ℃, collected by centrifugation, and lysed as described above to prepare crude extracts containing His-AGB1 or His-AGG1. Addition of IPTG was not necessary to express His-AGB1 or His-AGG1. His-AGB1 or His-AGG1 in the crude extracts was bound to Ni-NTA His-Bind resin (Novagen) following the manufacturer's instructions. The resin was washed 4 times by 1× TBS and resuspended in 250 mM imidazole to elute His-AGB1 or His-AGG1. The slurry was centrifuged at 6000 ×g for 2 min and the supernatant was used as purified His-AGB1 or His-AGG1 solution for the phosphatase assay. For a control, mVenus/pRSETB (Nagai *et al.*, 2002), which was obtained from the RIKEN Brain Science Institute, was introduced into BL21 (DE3) to express polyhistidine-tagged mVenus (His-mVenus). His-mVenus was expressed and purified as described above, and used for the phosphatase assay. The phosphatase assay was performed using a Non-Radioactive Serine–Threonine Phosphatase Assay System (Promega). To confirm the phosphatase activity of AtPP2C52, phosphatase reaction was performed in a volume of 50 μl containing 20 mM $MgCl_2$, 0.1 Mm phosphopeptide (RRApTVA), 50 mM Tris–HCl, pH 7.5, 1/20 (v/v) purified GST-AtPP2C52 with or without 20 mM EDTA. After 20 min incubation at room temperature, 50 μl of molybdate dye/additive solution was added to the solution, and the solution was incubated for another 20 min at room temperature to fully develop the color. A_{600} of the solution was measured and the amounts of the released phosphate were calculated by a standard curve obtained from known concentrations of phosphate standard solutions. For a negative control, GST alone was expressed as GST-AtPP2C52 and used for the assay instead of GST-AtPP2C52. To examine the effects of AGB1 and AGG1, the reaction was performed in a volume of 50 μl containing 20 mM $MgCl_2$, 0.1 mM phosphopeptide (RRApTVA), 1/20 (v/v) purified GST-AtPP2C52, 1/10 (v/v) purified His-AGB1, and

1/10 (v/v) His-AGG1. When one or both of His-AGB1 and His-AGG1 were not added, imidazole was added to make a final concentration of 50 mM. The amounts of the released phosphate were calculated as above.

4.3.10 RT-PCR

For RNA extraction, leaves, roots, flowers and flower stalks from mature plants and 2-week-old seedlings were sampled. Total RNA was prepared using RNeasy Plant Mini Kit (Qiagen) and cDNA was synthesized from 3 μg of the total RNA with PrimeScript Reverse Transcriptase (Takara Bio) using an oligo (dT) primer. The reaction mixtures were diluted 20 times with distilled water and used as a template for PCR. *PP2C52* expression was measured by real-time quantitative RT-PCR (qRT-PCR) using primers 5'-CTCGGCTGCGCGTGAATGGA-3' and 5'-TCACGCGTGTGACGCCTTGT-3', GoTaq qPCR Master Mix (Promega) and a StepOne Real-Time PCR System (Applied Biosystems). Relative expression levels were calculated by the comparative C_T method using *UBQ5* as an internal control gene.

4.4 Results

4.4.1 AtPP2C52 is a novel AGB1-interacting protein

Full-length AGB1 was used as the bait in the Y2H screen of the Arabidopsis leaf library. More than 3600 positive clones were obtained. 60–70% of these clones expressed AGG1. Among the non-AGG1 clones, approximately 400 clones were examined and two of them were a type-2C protein phosphatase (PP2C), AtPP2C52 (GenBank Accession NP_680572).

AtPP2C52 was a putative protein phosphatase and thought to catalyze protein dephosphorylation. AtPP2C52 is classified into group E PP2Cs in Arabidopsis (Xue *et al*., 2008). To examine the specificity of the AGB1-AtPP2C52 interaction, two other group E Arabidopsis PP2Cs, AtPP2C1 and AtPP2C74, as well as AtPP2C52, were subjected to an Y2H assay. AtPP2C52 enabled yeast cells to grow on the selection media when it was co-expressed with AGB1, but neither AtPP2C1 nor AtPP2C74 had the same effect (Fig. 4-1A), suggesting that AGB1 specifically interacts with AtPP2C52 in yeast cells.

To examine whether AtPP2C52 interacts with AGB1 *in vitro*, a GST pull-down assay was performed. GST-fused AtPP2C52 (GST-AtPP2C52) was bound to resin and mixed with a solution containing Myc-tagged AGB1 (Myc-AGB1). After incubation, GST-AtPP2C52 was eluted from the resin and Myc-AGB1 in the elutant was analyzed by immunoblotting. Specific signals of Myc-AGB1 were detected only when both AtPP2C52 and AGB1 were present (Fig.4-1B), indicating that AtPP2C52 interacts with AGB1 *in vitro*.

The interaction between AGB1 and AtPP2C52 was examined through a BiFC assay. The ORF of *AGB1* was fused downstream of the nYFP and the ORF of

AtPP2C52 was fused upstream of the cYFP. When nYFP-fused AGB1 and cYFP-fused AtPP2C52 were co-expressed in onion epidermal cell and Arabidopsis mesophyll protoplasts, BiFC signals were detected in the peripheral region of the cells (Fig. 4-1C,D), indicating that AGB1 and AtPP2C52 form a complex in the plasma membrane.

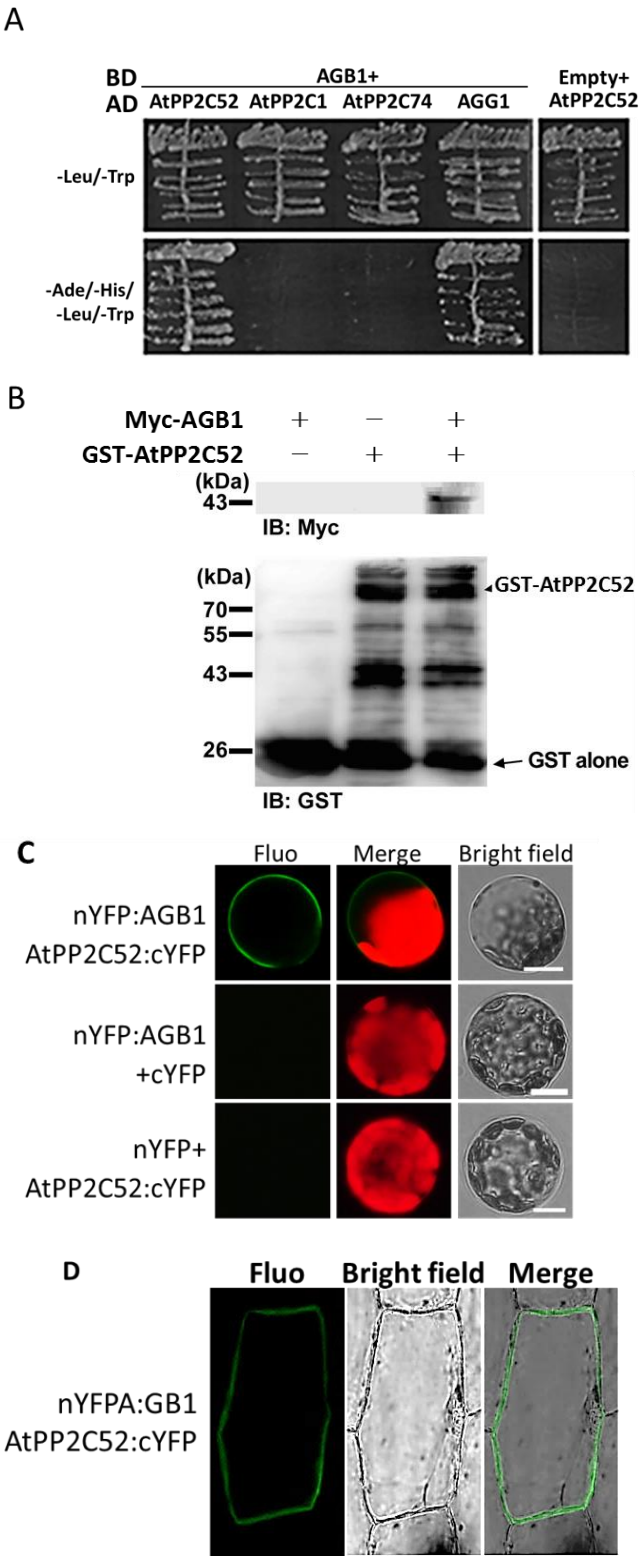

Fig. 4-1. Interaction between AtPP2C52 and AGB1. A, Y2H interactions between AGB1 and AtPP2C52 homologs. The ORF of *AGB1* was cloned into pGBKT7, and the ORFs of *AtPP2C52*, *AtPP2C1*, *AtPP2C74* and *AGG1* were cloned into pGADT7-rec. The pGBKT7-AGB1 and one of the pGADT7-rec constructs were co-transformed into the yeast strain AH109. Cells were grown

on control media and media lacking adenine and histidine (-His/-Ade). The combination of AGB1 + AGG1 is shown as a positive control. The combination of pGBKT7 empty vector (Empty) + AtPP2C52 is shown as a negative control. B. *In vitro* GST pull-down assay. GST-fused AtPP2C52 and Myc-tagged AGB1 were expressed in *E. coli* and used for the analysis. The presence or absence of each protein in the reaction mixture is shown as + or -, respectively. Experiments were performed 4 times and a representative result is shown. Antibodies used for immunoblotting are shown as IB: Myc and IB: GST. C, BiFC assays in Arabidopsis protoplasts, Bar=25μm. D, BiFC assays in onion epidermal cells. Bar=100μm. nYFP:AGB1 + cYFP, and nYFP + AtPP2C52:cYFP were used as negative controls to show that these proteins cannot interact with half-YFP. Fluo: fluorescence from YFP or GFP. Merge: overlap of Bright field and Fluo signal.

4.4.2 AtPP2C52 is localized in the plasma membrane via myristoylation

Subcellular localization of AtPP2C52 was examined using AtPP2C52 which was GFP-tagged in its C-terminus (AtPP2C52:GFP). When expressed in onion epidermal cells (Fig. 4-2A, lower panels) and Arabidopsis protoplast (Fig. 4-2B, lower panels), the fluorescence of AtPP2C52:GFP fusion protein was observed in the peripheral region of the cells, suggesting that AtPP2C52 protein is located in the plasma membrane.

A motif scanning program (Myristoylator, http://web.expasy.org/myristoylator/) predicted that the N terminus of AtPP2C52 is myristoylated. Myristoylation is the process of adding a C: 14 fatty acid, myristate, to the N-terminal glycine of a subset of proteins and thus enhances their plasma membrane localization (Resh, 1999). To examine whether myristoylation is responsible for the plasma membrane localization of AtPP2C52, the effects of substitution of the glycine residue at position 2, which is the putative myristoylation site of AtPP2C52, with an alanine residue were examined. The fluorescence of mutated AtPP2C52:GFP was detected in the nucleus but not in the plasma membrane (Fig. 4-2C, right panel), suggesting that myristoylation is necessary for the plasma membrane localization of AtPP2C52. A motif-scanning program (cNLS Mapper, http://nls-mapper.iab.keio.ac.jp/cgi-bin/NLS_Mapper_form.cgi, Kosugi *et al*. 2009) predicted that the N-terminal region (position 34-63) of AtPP2C52 acts as a nuclear localization signal, supporting the idea that AtPP2C52 is localized to the nucleus when it is not myristoylated. To examine whether AGB1 affects the subcellular localization of AtPP2C52, AtPP2C52:GFP was expressed in mesophyll protoplasts from an AGB1-null mutant, *agb1-2* (Ullah *et al*. 2003). The fluorescence of AtPP2C52:GFP was detected in the cell periphery in the *agb1-2* protoplasts as well as in wild-type protoplasts (Fig. 4-2D lower panel), suggesting that AGB1 does not regulate the subcellular localization of AtPP2C52.

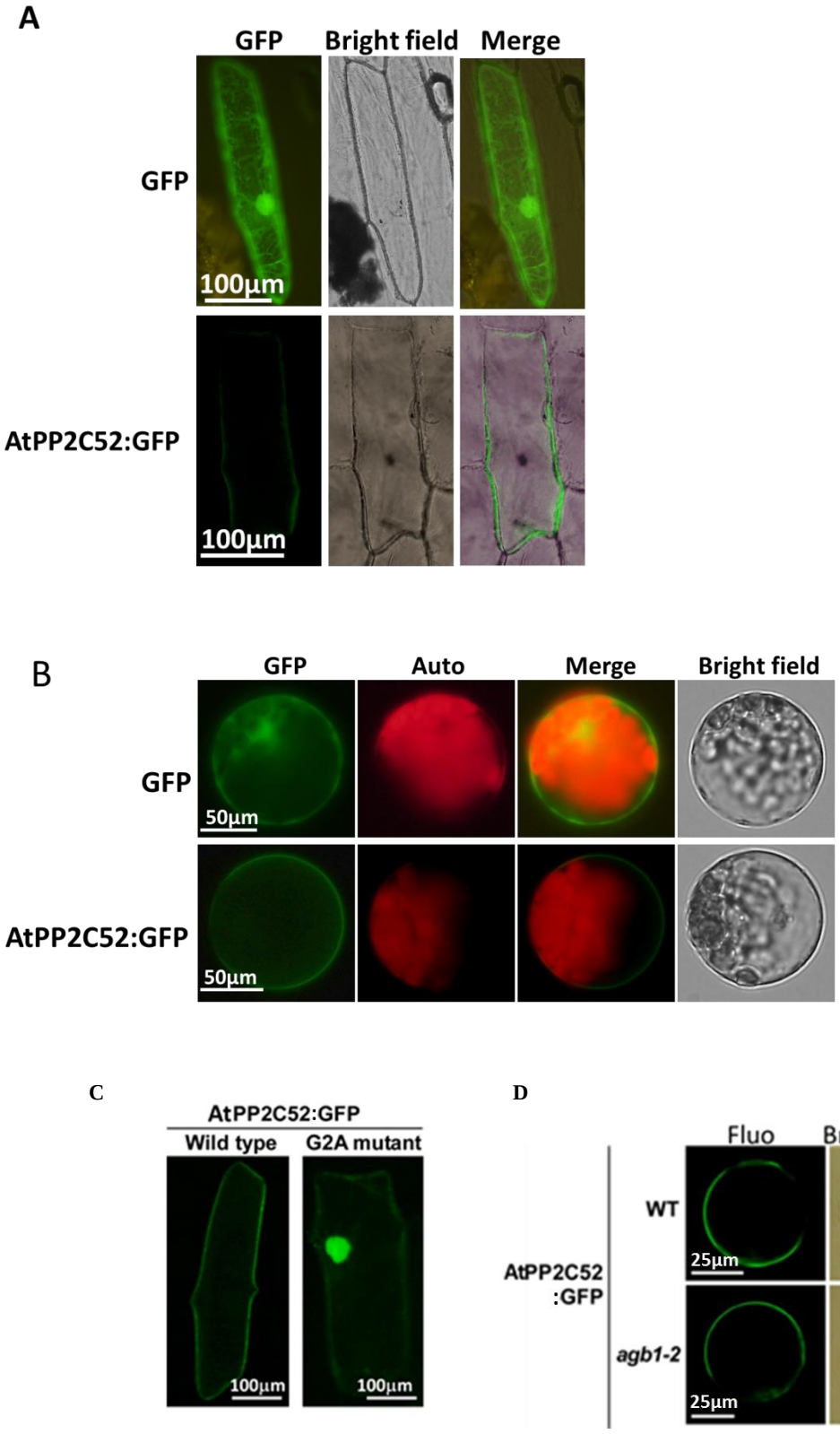

Fig. 4-2. Subcellular localization of AtPP2C52. A, Localization of AtPP2C52 in onion epidermal cells. Merge: overlap of Bright field and GFP signal. B, Localization of AtPP2C52 in Arabidopsis protoplasts. Auto, chlorophyll. Merge: overlap of Auto and GFP signal. C. Wild-type

AtPP2C52 or its G2A mutant, which has a glycine → alanine substitution at position 2, was expressed as a GFP-fusion protein. D, AtPP2C52:GFP was expressed in Arabidopsis mesophyll protoplasts isolated from wild type or *agb1-2*. Fluo: fluorescence from GFP.

4.4.3 Site-directed mutations abolished the interaction between AtPP2C52 and AGB1

Three AtPP2C52 mutants (AtPP2C52^{G99D}, AtPP2C52^{G105D} and AtPP2C52$^{DGH102\text{-}104ERN}$) were generated because their high conservation in PP2Cs (Fig. 4-3A) and their involvement in the PP2C active site (Das *et al*., 1996; Sheen, 1998). The mutated sequences encoded unrelated amino acids. These mutant proteins were expressed by TNT Quick Coupled Transcription/Translation Systems (Promega) and used for western blotting. As a result, none of these mutations of affected the molecular weight of these mutant proteins (Fig. 4-3B). However, all of these mutations abolished the interaction between AGB1 and AtPP2C52 (Fig. 4-3C), suggesting these sites are necessary for the interaction between AGB1 and AtPP2C52.

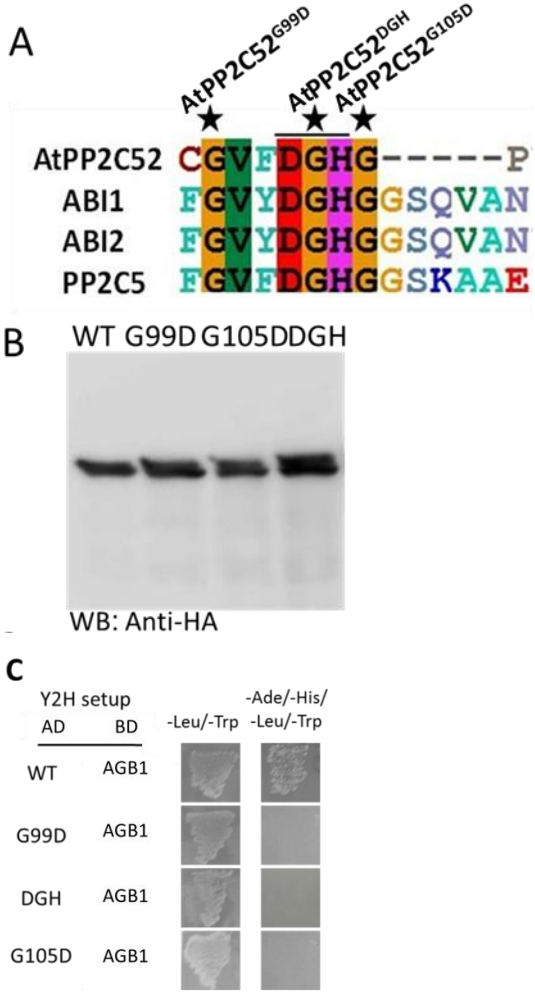

Fig. 4-3. Site-directed mutations abolished the interaction between AtPP2C52 and AGB1. A, AtPP2C52, ABI1 (At4g26080), ABI2 (At5g57050), and PP2C5 (AT2G40180) possess two uniquely conserved G residues around the DGH (underlined) active site. B, Proteins were expressed by TNT Quick Coupled Transcription/Translation Systems and separated by SDS/PAGE. Anti-HA antibody was used. C, Y2H analysis. In yeast cells that cannot grew on quadruple dropout medium (SD/-Ade/-His/-Leu/-Trp), the reporter genes cannot be activated when the bait (BD:AGB1) interacted with the prays. AD:AtPP2C52^{G99D}: G99D. AD:AtPP2C52^{G105D}: G105D. AD:AtPP2C52$^{DGH102\text{-}104ERN}$: DGH).

4.4.4 Stage and tissue specificity of AtPP2C52 expression

To check the temporal-spatial expression pattern of *AtPP2C52*, transgenic plants expressing a promoter-reporter fusion gene ($P_{AtPP2C52}$::*GUS*) were used. $P_{AtPP2C22}$::*GUS* was expressed in almost all the plant organs (Fig. 4-4). In 4-day-old seedlings, $P_{AtPP2C52}$::*GUS* was predominantly expressed in vascular, root tip and apical meristem (Fig. 4-4A,B). In 3-week-old plants, $P_{AtPP2C52}$::*GUS* was evident in the whole plant (Fig. 4-4C). Obviously, $P_{AtPP2C52}$::*GUS* transcript level was still higher in vascular and apical meristem. In adult plant, $P_{AtPP2C52}$::*GUS* was expressed in all the organs of flower, excepting the anther (Fig. 4-4D-F). The expression level of $P_{AtPP2C52}$::*GUS* was lower in the sporangia (Fig. 4-4G,H).

The transcript levels of *AtPP2C52* in various tissues were confirmed by real-time quantitative RT-PCR. *AtPP2C52* mRNA expression was also detected in all the tissues studied, being highest in flower stalks and lowest in seedlings (Fig. 4-4I).

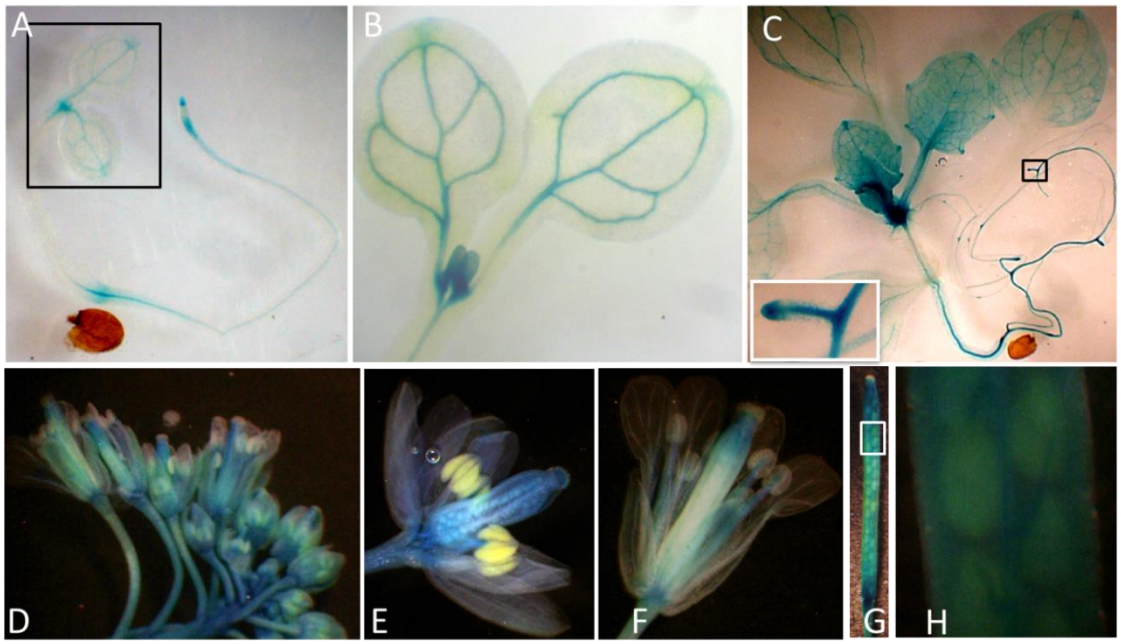

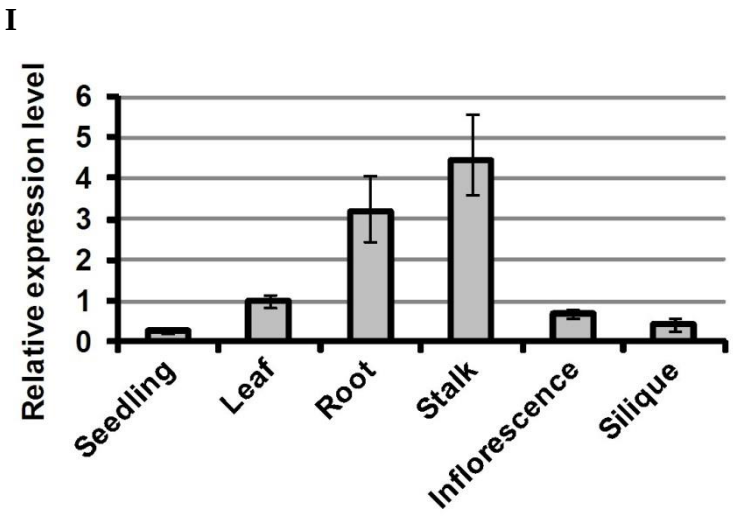

Fig. 4-4. Temporal and spatial expression of *AtPP*2C52. A, GUS staining showing the expression of $P_{AtPP2C52}$::GUS in 4-day-old seedlings cultured under SDs. B. Enlarged view indicated by blank rectangle in A. C, Three-week-old plants cultured under SDs. D, Inflorescence. E and F, Flower at stage 12 and 15. G, Silique. H, Enlarged view indicated by white rectangle in G. I，Real-time quantitative RT-PCR analysis of *AtPP2C52* transcripts in various Arabidopsis tissues. Relative expression levels were calculated by the comparative C_T method using *UBQ5* as an internal control gene and leaf sample as a reference sample. Experiments were performed in triplicate. Values are means ± SE.

4.4.5 AtPP2C52 has protein phosphatase activity

To determine whether AtPP2C52 functions as a protein phosphatase, an *in vitro* phosphatase assay was performed using purified GST-AtPP2C52. Phosphate was released from a phosphorylated substrate when GST-AtPP2C52 was present in the reaction solution. Mg^{2+} is a cofactor required for PP2C activity. As expected, removal of Mg^{2+} by EDTA inhibited the phosphate release (Fig. 4-5 A). These results suggest that AtPP2C52 has protein phosphatase activity *in vitro*. Because AtPP2C52 physically interacts with AGB1 and is a possible effector regulated by Gβγ, the effects of AGB1 and AGG1 on the activity of AtPP2C52 were examined using purified polyhistidine-tagged AGB1 and AGG1 (His-AGB1 and His-AGG1, respectively). However, a combination of AGB1 and AGG1 did not significantly change the activity of AtPP2C52 (Fig. 4-5 B).

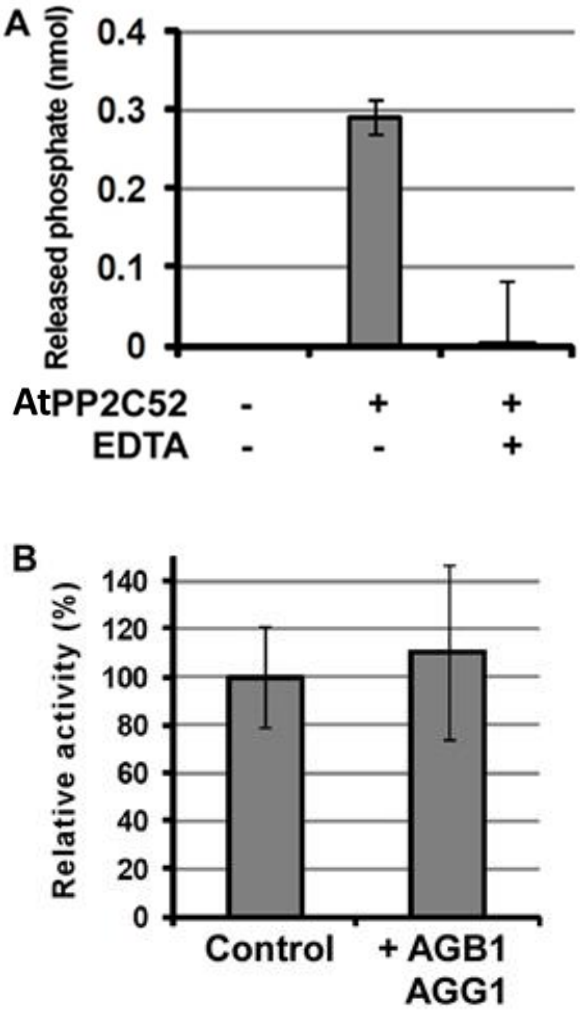

Fig. 4-5. *In vitro* phosphatase assay. A, Confirmation of the phosphatase activity of AtPP2C52. GST-fused AtPP2C52 was expressed in *E. coli*, purified and used for analysis. Phosphatase reactions were performed in the presence or absence of 20 mM EDTA (EDTA + or EDTA -, respectively). For AtPP2C52 -, GST alone was used for the reaction. Experiments were performed in triplicate. Values are means ± SE. B, Effects of AGB1 and AGG1 on the phosphatase activity of AtPP2C52. AGB1 and AGG1 were expressed as polyhistidine-tagged proteins in *E. coli*, purified and used for analysis. Both of them were added to the phosphatase reaction mixture (shown as + AGB1 AGG1). For Control, polyhistidine-tagged mVenus (a variant of GFP) was added to the reaction mixture. Experiments were performed in triplicate. Values are means ± SE.

4.4.6 Potential substrates of AtPP2C52

To further identify signaling compartments of the signaling pathway mediated by AtPP2C52, full-length AtPP2C52 was used as the bait in the Y2H screening. Even on high-stringency selection media, which lack histidine and adenine, more than 2500 positive clones were obtained. Among them, 300 clones were examined. Some AtPP2C52-interacting proteins were identified (Table 4-1).

A proteasome maturation factor, UMP1 (At5G38650), and a cysteine proteinase, RD21a (At1G47128), were used for further analysis. Y2H interaction of AtPP2C52 with either UMP1 or RD21a was confirmed (Fig. 4-6A,B). AtPP2C52^{G99D} and AtPP2C52$^{DGH102\text{-}104ERN}$ failed to interact with UMP1 in Y2H (Fig. 4-6A). G105D mutations did not affect the Y2H interaction between AtPP2C52 and UMP1 (Fig. 4-6A). All of these mutations abolished the Y2H interaction between AtPP2C52 and RD21a (Fig. 4-6B).

The interactions were examined by a BiFC assay in Arabidopsis protoplast. The ORFs of *UMP1* and *RD21a* were fused downstream of the nYFP. BiFC signals of nYFP-fused UMP1 and cYFP-fused AtPP2C52 were also detected in the peripheral region (Fig. 4-6C), suggesting that AtPP2C52 interacted with UMP1 in the plasma membrane. AtPP2C52 interacted with RD21a not only in the plasma membrane but also in the nucleus (Fig. 4-6C). These results suggest that RD21a and UMP1 are the potential substrates of AtPP2C52.

Table 4-1. AtPP2C52-interacting proteins identified by Y2H assay.

Gene identifier	Gene symbol	Gene description	localization	Summary	amino acid(aa)
AT1G01470	LEA14	putative desiccation-related protein LEA14	cytosol	Response to wounding and light stress and might be involved in protection against dessication	151
AT1G47128	RD21	cysteine proteinase RD21a	apoplast, chloroplast, plasmodesma, vacuole	Cysteine-type endopeptidase activity, cysteine-type peptidase activity, protein binding	462
AT5G38650	UMP1	Proteasome maturation factor UMP1	unknown	Proteasome maturation factor UMP1	141
AT1G67250	UMP1	Proteasome maturation factor UMP1	unknown	Proteasome maturation factor UMP1	141
AT3G11700	FLA18	FASCICLIN-like arabinogalactan protein 18 precursor	vacuole	Response to cyclopentenone, cell adhesion	462
AT4G03520	ATHM2	chloroplast localized thioredoxin, similar to prokaryotic types	chloroplast, chloroplast stroma, chloroplast thylakoid membrane, thylakoid	positive regulation of catalytic activity, response to oxidative stress	72
AT3G46000	ADF2	actin depolymerizing factor 2.	cytoplasm, intracellular, nucleus, plasma membrane	actin binding	137
AT3G52370	FLA15	FASCICLIN-like arabinogalactan protein 15 precursor	endomembrane system	cell adhesion	436
AT1G20110	T20H2.10	RING/FYVE/PHD zinc finger superfamily protein	unknown	signal transduction, phosphoinositide binding	601
AT2G30110	UBA1	ubiquitin-activating enzyme E1 1	cytosol, plasma membrane, plasmodesma	ubiquitin activating enzyme activity, ubiquitin-protein ligase activity	1080
AT1G09070	SRC2	SOYBEAN GENE REGULATED BY COLD-2	endoplasmic reticulum, protein storage vacuole	protein targeting to vacuole, protein binding	324
AT3G01090	SNF1	SNF1-related protein kinase	nuclear ubiquitin ligase complex	Protein binding, ABA signaling pathway	512
AT5G05440	PYL5	Pyrabactin resistance 1-like 5	cellular component, cytoplasm, nucleus	abscisic acid mediated signaling pathway	203

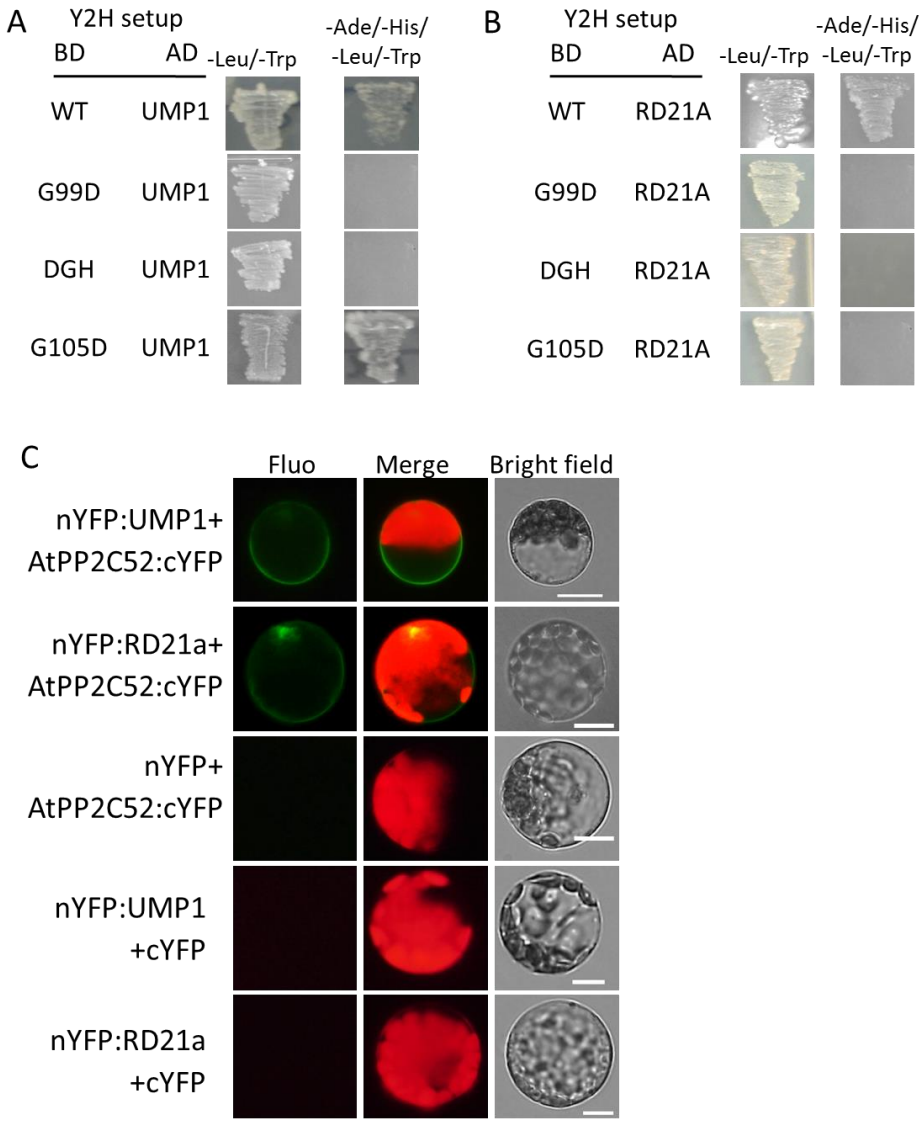

Fig. 4-6. AtPP2C52 interacted with UMP1 and RD21a. A and B, Y2H. In yeast cells that cannot grew on quadruple dropout medium (SD/-Ade/-His/-Leu/-Trp), the reporter genes cannot be activated when the baits (BD) interacted with the pray (AD). Wild-type AtPP2C52: WT. $AtPP2C52^{G99D}$: G99D. $AtPP2C52^{G105D}$: G105D. $AtPP2C52^{DGH102\text{-}104ERN}$: DGH. C, BiFC assays in Arabidopsis protoplasts. The combinations of nYFP:AGB1 + cYFP, nYFP +AtPP2C52:cYFP, nYFP:UMP1 + cYFP, and nYFP:RD21a + cYFP were used as negative controls to show that these proteins cannot interact with half-YFP. Scale bar=25μm.

4.5 Discussion

AtPP2C52 is highly similar to another putative myristoylated AtPP2C, AtPP2C74 (similarities: 62%). AtPP2C52 enabled yeast cells to grow on the selection media when it was co-expressed with AGB1, but neither AtPP2C1 nor AtPP2C74 had the same effect (Fig. 4-1A), suggesting that AGB1 specifically interacts with PP2C52 in yeast cells. Meanwhile, AtPP2C52 interacts with AGB1 *in vitro* (Fig. 4-1B).

AtPP2C52 is localized in the plasma membrane. The fluorescence of PP2C52:GFP was detected in the cell periphery in the *agb1-2* protoplasts as well as in wild-type protoplasts (Fig. 4-2D), suggesting that AGB1-deficiency does not affect the subcellular localization of AtPP2C52. AGB1 is known to be localized in the plasma membrane and the nucleus (Anderson and Botella, 2007). BiFC signal of AGB1 and AtPP2C52 was observed in the cell periphery (Fig. 4-1B), indicating that AGB1 and AtPP2C52 form a complex in the plasma membrane.

AtPP2C52 has protein phosphatase activity. However, a combination of AGB1 and AGG1 did not significantly change the activity of AtPP2C52. It is possible that AGB1 serves as a scaffold to broaden the substrate range of AtPP2C52.

ARABIDOPSIS SNF1 KINASE HOMOLOG 10 (AKIN10, AT3g01090) which are catalytic α subunits of the SNF1 kinase complex, was identified as a AtPP2C52-interacting protein (Table 4-1). SNF1 can be localized to the plasma membrane via myristoylation of its β subunits, AKINβ1 and AKINβ2 (Pierre *et al.*, 2007). SNF1 has been suggested to positively regulate sugar- and ABA-responsive pathways (Baena-González *et al.*, 2007; Jossier *et al.*, 2009). Activation of SNF1 requires phosphorylation of its α subunits (Sugden *et al.*, 1999; Shen *et al.*, 2009). Therefore it is possible that AtPP2C52 dephosphorylates AKIN10 and AKIN11, and thereby inactivates SNF1 and the subsequent sugar- and ABA-responsive pathways.

AGB1 may promote the AtPP2C52-mediated inactivation of SNF1. This idea is consistent with previous studies suggesting that AGB1 is a negative regulator of sugar- and ABA-responsive pathways (Chen *et al.*, 2004).

In conclusion, this study has revealed that AtPP2C52 interacts with AGB1 AtPP2C52 is a putative myristoylated protein and localized in the plasma membrane, where Gβγ is present (Adjobo-Hermans *et al.*, 2006). AtPP2C52 is a strong candidate for the effector regulated by Gβγ in Arabidopsi

Conclusions

Heterotrimeric G proteins (Gα, Gβ, Gγ) play important roles in signal transduction among various eukaryotic species. G proteins transmit signals by regulating the activities of effector proteins, but only a few Gβ-interacting effectors have been identified in plants. In this study, AtRBM22 and AtPP2C52 were identified as novel Gβ (AGB1)-interacting partners.

- AtRBM22 interacts with AGB1 in nuclear speckles. AGB1 played a role in the translocation of AtRBM22 into nuclear speckles. Translocation of AtRBM22 into nuclear speckles is mediated by multiple proteins other than AGB1. *AtRBM22* gene was predominantly expressed in pollen by GUS staining. *atrbm22* mutation caused early flowering. Abnormal flower phenotypes and reduced seed production were found in the AtRBM22 overexpressing plants. These results suggest that AtRBM22 plays multiple roles in the development of Arabidopsis.

- AtPP2C52, which is widely expressed in plant, is a potential effector of AGB1 in the plasma membrane in Arabidopsis. AtPP2C52 has localized in the plasma membrane via myristoylation. AtPP2C52 has protein phosphatase activity. The activity of AtPP2C52 is not affected by AGB1 or the Gγ subunit, AGG1. In addition, some potential substrate of AtPP2C52 was identified.

References

Addepalli B, Hunt AG (2008) Ribonuclease activity is a common property of Arabidopsis CCCH-containing zinc-finger proteins. FEBS Lett 582: 2577-2582.

Adjobo-Hermans MJW, Goedhart J, Gadella TWJ (2006) Plant G protein heterotrimers require dual lipidation motifs of Galpha and Ggamma and do not dissociate upon activation. Journal of cell science 119: 5087-5097.

Ajuh P, Kuster B, Panov K, Zomerdijk JC, Mann M, Lamond AI (2000) Functional analysis of the human CDC5L complex and identification of its components by mass spectrometry. EMBO J 19: 6569-6581.

Anderson DJ, Botella JR (2007) Expression analysis and subcellular localization of the *Arabidopsis thaliana* G-protein β-subunit AGB1. Plant Cell Rep 26: 1469-1480.

Baena-González E, Rolland F, Thevelein JM, and Sheen J (2007) A central integrator of transcription networks in plant stress and energy signalling. Nature 448: 938-942.

Beffa R, Szell M, Meuwly P, Pay A, Vögeli-Lange R, Métraux JP, Neuhaus G, Meins F Jr, Nagy F (1995) Cholera toxin elevates pathogen resistance and induces pathogenesis-related gene expression in tobacco. EMBO J 14: 5753-5761.

Bevan MW (1984) Binary Agrobacterium vectors for plant transformation. Nucleic Acids Res 12: 8711-8721.

Black DL (2003) Mechanisms of alternative pre-messenger RNA splicing. Annu Rev Biochem 72: 291-336.

Black DL, Grabowski PJ (2003) Alternative pre-mRNA splicing and neuronal function. Prog Mol Subcell Biol 31: 187-216.

Blencowe BJ (2006) Alternative splicing: new insights from global analyses. Cell 126: 37-47.

Burd CG, Dreyfuss G (1994) Conserved structures and diversity of functions of RNA-binding proteins. Science 265: 615-621.

Casey PJ (1995) Mechanisms of protein prenylation and role in Gprotein function.

Biochem Soc Trans 23: 161-166.

Chakravorty D, Trusov Y, Botella JR (2012) Site-directed mutagenesis of the Arabidopsis heterotrimeric G: protein β subunit suggests divergent mechanisms of effector activation between plant and animal G proteins. Planta 235: 615-627.

Chakravorty D, Trusov Y, Zhang W, Acharya BR, Sheahan MB, McCurdy DW, Assmann SM, Botella JR. (2011) An atypical heterotrimeric G-protein γ-subunit is involved in guard cell K^+-channel regulation and morphological development in *Arabidopsis thaliana*, Plant J. 67: 840-851.

Chen JG, Gao Y, Jones AM (2006) Differential roles of Arabidopsis heterotrimeric G-protein subunits in modulating cell division in roots. Plant Physiol 141: 887-897.

Chen JG, Pandey S, Huang J, Alonso JM, Ecker JR, Assmann SM, Jones AM (2004) GCR1 can act independently of heterotrimeric G-protein in response to brassinosteroids and gibberellins in Arabidopsis seed germination. Plant Physiol 135: 907-915.

Cheng Y, Kato N, Wang W, Li J, Chen X (2003) Two RNA binding proteins, HEN4 and HUA1, act it the processing of AGAMOUS pre-RNA in *Arabidopsis thaliana*. Dev Cell 4: 53-66.

Christmann A, Moes D, Himmelbach A, Yang Y, Tang Y, Grill E (2006) Integration of abscisic acid signalling into plant responses. Plant Biol (Stuttg) 8: 314-825.

Clough SJ, Bent AF (1998) Floral dip: a simplified method for Agrobacterium-mediated transformation of *Arabidopsis thaliana.* Plant J 16: 735-743.

Cohen P (1989) The structure and regulation of protein phosphatases. Annu Rev Biochem 58: 453-508.

Cohen PT (1997) Novel protein serine/threonine phosphatases: variety is the spice of life. Trends Biochem Sci 22: 245-251.

Cole GM, Reed SI (1991) Pheromone-induced phosphorylation of a G protein β subunit in *S. cerevisiae* is associated with an adaptive response to mating pheromone, Cell 64: 703-716.

Das AK, Helps NR, Cohen PTW, Barford D (1996) Crystal structure of the protein serine/threonine phosphatase 2C at 2.0 Å resolution. EMBO J 15: 6798-6809.

Dye BT and Patton JG. (2001) An RNA recognition motif (RRM) is required for the localization of PTB-associated splicing factor (PSF) to subnuclear speckles. Exp Cell Res 263: 131-144.

Fairley-Grenot K, Assmann SM (1991) Evidence for G-protein regulation of inward K^+ channel current in guard cells of fava bean. Plant Cell 3: 1037-1044.

Fakan S, Leser G, Martin TE (1984) Ultrastructural distribution of nuclear ribonucleoproteins as visualized by immunocytochemistry on thin sections. J Cell Bio 98: 358-363.

Fang Y, Hearn S, Spector DL (2004) Tissue-specific expression and dynamic organization of SR splicing factors in Arabidopsis. Mol Biol Cell 15: 2664-2673.

Filichkin SA, Priest HD, Givan SA, Shen R, Bryant DW, Fox SE, Wong WK, Mockler TC (2010) Genome-wide mapping of alternative splicing in *Arabidopsis thaliana*. Genome Res 20: 45-58.

Fornara F, de Montaigu A, Coupland G, SnapShot (2010) Control of flowering in Arabidopsis, Cell. 141 550.e1-2.

Friedman EJ, Wang HX, Jiang K, Perovic I, Deshpande A, Pochapsky TC, Temple BR, Hicks SN, Harden TK, Jones AM (2011) Acireductone dioxygenase 1 (ARD1) is an effector of the heterotrimeric G protein beta subunit in Arabidopsis. J Biol Chem 286: 30107-30118.

Fujii H, Verslues PE, Zhu J (2007) Identification of two protein kinases required for abscisic acid regulation of seed germination, root growth, and gene expression in Arabidopsis. Plant Cell 19: 485-494.

Gether U (2000) Uncovering molecular mechanisms involved in activation of G protein coupled receptors. Endocr Rev 21: 90-113.

Gotta M, Ahringer J (2001) Distinct roles for Galpha and Gbetagamma in regulating spindle position and orientation in Caenorhabditis elegans embryos. Nat Cell Biol 3: 297-300.

Graveley BR (2001) Alternative splicing: increasing diversity in the proteomic world, Trends Genet. 17: 100-107.

Hampoelz B, Knoblich JA (2004) Heterotrimeric G proteins: new tricks for an old dog. Cell 119: 453-456.

Hartmuth K, Urlaub H, Vornlocher HP, Will CL, Gentzel M, Wilm M, Lührmann R (2002) Protein composition of human prespliceosomes isolated by a tobramycin affinity-selection method. Proc Natl Acad Sci U S A 99: 16719-16724.

He F, Wang CT, Gou LT (2009) RNA-binding motif protein RBM22 is required for normal development of zebrafish embryos. Genet Mol Res 8: 1466-1473.

Hirayama T, Shinozaki K (2007) Perception and transduction of abscisic acid signals: Keys to the function of the versatile plant hormone ABA. Trends Plants Sci 12: 343-351.

Hjerrild M, Gammeltoft S (2006) Phosphoproteomics toolbox: computational biology, protein chemistry and mass spectrometry. FEBS Lett 580: 4764-4770.

Hunter T (1998) The Croonian lecture 1997. The phosphorylation of proteins on tyrosine: its role in cell growth and disease. Philos. Trans. R. Soc. Lond. B Biol. Sci. 353: 583-605.

Ishida S, Takahashi Y, Nagata T (1993) Isolation of cDNA of an auxin-regulated gene encoding a G protein beta subunit-like protein from tobacco BY-2 cells. Proc Natl Acad Sci U S A 90: 11152-11156.

Jang S, Torti S, Coupland G (2009) Genetic and spatial interactions between FT, TSF and SVP during the early stages of floral induction in Arabidopsis. Plant J 60: 614-625.

Janowicz A, Michalak M, Krebs J (2011) Stress induced subcellular distribution of ALG-2, RBM22 and hSlu7. Biochimica et Biophysica Acta 1813: 1045-1049.

Johnson JM, Castle J, Garrett-Engele P, Kan Z, Loerch PM, Armour CD, Santos R,

Schadt EE, Stoughton R, Shoemaker DD (2003) Genome-wide survey of human alternative pre-mRNA splicing with exon junction microarrays. Science 302: 2141-2144.

Jones AM, Assmann SM (2004) Plants: the latest model system for G-protein research. EMBO Rep 5: 572-578.

Jones HD, Smith SJ, Desikan R, Plakidou-Dymock S, Lovegrove A, Hooley R (1998) Heterotrimeric G proteins are implicated in gibberellin induction of a-amylase gene expression in wild oat aleurone. Plant Cell 10: 245-254.

Jossier M, Bouly JP, Meimoun P, Arjmand A, Lessard P, Hawley S, Grahame Hardie D, and Thomas M (2009) SnRK1 (SNF1-related kinase 1) has a central role in sugar and ABA signalling in *Arabidopsis thaliana*. Plant J 59: 316-328.

Jovtchev G, Schubert V, Meister A, Barow M, Schubert I (2006) Nuclear DNA content and nuclear and cell volume are positively correlated in angiosperms. Cytogenet Genome Res 114: 77-82.

Kato C, Mizutani T, Tamaki H, Kumagai H, Kamiya T, Hirobe A, Fujisawa Y, Kato H, Iwasaki Y (2004) Characterization of heterotrimeric G protein complexes in rice plasma membrane. Plant J 38: 320-331.

Kerk D, Bulgrien J, Smith DW, Barsam B, Veretnik S, Gribskov M. (2002) The complement of protein phosphatase catalytic subunits encoded in the genome of Arabidopsis. Plant Physiol 129: 908-925.

Kilian J, Whitehead D, Horak J, Wanke D, Weinl S, Batistic O, D'Angelo C, Bornberg-Bauer E, Kudla J, Harter K. (2007) The AtGenExpress global stress expression data set: protocols, evaluation and model data analysis of UV-B light, drought and cold stress responses. Plant J 50: 347-363.

Kittler R, Putz G, Pelletier L, Poser I, Heninger AK, Drechsel D, Fischer S, Konstantinova I, Habermann B, Grabner H, Yaspo ML, Himmelbauer H, Korn B, Neugebauer K, Pisabarro MT, Buchholz F (2004) An endoribonuclease-prepared siRNA screen in human cells identifies genes essential for cell division Nature. 432: 1036-1040.

Klopffleisch K, Phan N, Augustin K, Bayne RS, Booker KS, Botella JR, Carpita NC, Carr T, Chen JG, Cooke TR, Frick-Cheng A, Friedman EJ, Fulk B, Hahn MG, Jiang K, Jorda L, Kruppe L, Liu C, Lorek J, McCann MC, Molina A, Moriyama EN, Mukhtar MS, Mudgil Y, Pattathil S, Schwarz J, Seta S, Tan M, Temp U, Trusov Y, Urano D, Welter B, Yang J, Panstruga R, Uhrig JF, Jones AM. (2011) Arabidopsis G-protein interactome reveals connections to cell wall carbohydrates and morphogenesis. Mol Syst Biol 7: 532.

Kobayashi S, Tsugama D, Liu S, Takano T (2012) A U-Box E3 ubiquitin ligase, PUB20, interacts with the Arabidopsis G-protein β subunit, AGB1. PLoS One. 7:e49207.

Kosugi S, Hasebe M, Tomita M, Yanagawa H (2009) Systematic identification of yeast cell cycle-dependent nucleocytoplasmic shuttling proteins by prediction of composite motifs, Proc. Natl. Acad. Sci. U. S. A. 106: 10171-10176.

Krebs EG, Beavo JA. (1979) Phosphorylation-dephosphorylation of enzymes. Annu Rev Biochem 48: 923-959.

Krebs J (2009) The influence of calcium signaling on the regulation of alternative splicing. Biochim Biophys Acta 1793: 979-984.

Krizek BA, Fletcher JC, (2005) Molecular mechanisms of flower development: an armchair guide, Nat Rev Genet 6: 688-698.

Krizek BA, Lewis MW, Fletcher JC (2006) RABBIT EARS is a second-whorl repressor of AGAMOUS that maintains spatial boundaries in Arabidopsis flowers. Plant J 45: 369-383.

Labadorf A, Link A, Rogers MF, Thomas J, Reddy AS, Ben-Hur A (2010) Genome-wide analysis of alternative splicing in Chlamydomonas reinhardtii. BMC Genomics 11: 114-123.

Lai WS, Carballo E, Strum JR, Kennington EA, Phillips RS, Blackshear PJ (1999) Evidence that tristetraprolin binds to AU-rich elements and promotes the deadenylation and destabilization of tumor necrosis factor alpha mRNA. Mol Cell Biol 19: 4311-4323.

Lai WS, Carballo E, Thorn JM, Kennington EA, Blackshear PJ (2000) Interactions of CCCH zinc finger proteins with mRNA. Binding of tristetraprolin-related zinc finger proteins to Au-rich elements and destabilization of mRNA. J Biol Chem 275: 17827-17837.

Lai WS, Parker JS, Grissom SF, Stumpo DJ, Blackshear PJ (2006) Novel mRNA targets for tristetraprolin (TTP) identified by global analysis of stabilized transcripts in TTP-deficient fibroblasts. Mol Cell Biol 26: 9196-9108.

Lai WS, Stumpo DJ, Blackshear PJ (1990) Rapid insulin-stimulated accumulation of an mRNA encoding a proline-rich protein. J Biol Chem 265: 16556-16563.

Lammers T, Lavi S (2007) Role of type 2C protein phosphatases in growth regulation and in cellular stress signaling. Crit Rev Biochem Mol Biol 42: 437-461.

Lander ES *et al*. (2001) Initial sequencing and analysis of the human genome, Nature 409: 860-921.

Lee JH, Park SH, Lee JS, Ahn JH (2007) A conserved role of SHORT VEGETATIVE PHASE (SVP) in controlling flowering time of Brassica plants. Biochim Biophys Acta 1769: 455-461.

Leung J, Bouvier-Durand M, Morris PC, Guerrier D, Chefdor F, Giraudat J (1994) Arabidopsis ABA response gene ABI1: features of a calcium-modulated protein phosphatase. Science 264: 1448-1452.

Leung J, Giraudat J (1998) Abscisic Acid Signal Transduction. Annu Rev Plant Physiol Plant Mol Biol 49: 199-222.

Leung J, Merlot S, Giraudat J (1997) The Arabidopsis ABSCISIC ACIDINSENSITIVE2 (ABI2) and ABI1 genes encode homologous protein phosphatases 2C involved in abscisic acid signal transduction. The Plant cell 9: 759-771.

Levy DL, Heald R (2010) Nuclear size is regulated by importin α and Ntf2 in Xenopus. Cell 143: 288-298.

Li J, Jia D, Chen X (2001) HUA1, a regulator of stamen and carpel identities in Arabidopsis, codes for a nuclear RNA binding protein. Plant Cell 13: 2269-2681.

Lin PC, Pomeranz MC, Jikumaru Y, Kang SG, Hah C, Fujioka S, Kamiya Y, Jang JC (2011) The Arabidopsis tandem zinc finger protein AtTZF1 affects ABA- and GA-mediated growth, stress and gene expression responses. Plant J 65: 253-268.

Lorković ZJ, Barta A (2002) Genome analysis: RNA recognition motif (RRM) and K homology (KH) domain RNA-binding proteins from the flowering plant *Arabidopsis thaliana*. Nucleic Acids Res 30: 623-635.

Lorković ZJ, Lehner R, Forstner C, Barta A (2005) Evolutionary conservation of minor U12-type spliceosome between plants and humans. RNA 11: 1095-1107.

Lu T, Lu G, Fan D, Zhu C, Li W, Zhao Q, Feng Q, Zhao Y, Guo Y, Li W, Huang X, Han B (2010) Function annotation of the rice transcriptome at single-nucleotide resolution by RNA-seq. Genome Res 20: 1238-1249.

Ma Y, Szostkiewicz I, Korte A, Moes D, Yang Y, Christmann A, Grill E (2009) Regulators of PP2C phosphatase activity function as abscisic acid sensors. Science 324: 1064-1068.

Malbon CC (2005) G proteins in development. Nat Rev Mol Cell Biol 6: 689-701

Mason MG, Botella JR (2000) Completing the heterotrimer: Isolation and characterization of an *Arabidopsis thaliana* G protein γ-subunit cDNA. Proc Natl Acad Sci U S A 97: 14784-14788.

Mason MG, Botella JR (2001) Isolation of a novel G-protein γ-subunit from *Arabidopsis thaliana* and its interaction with Gβ. Biochim Biophys Acta 1520: 147-153.

Merlot S, Gosti F, Guerrier D, Vavasseur A, Giraudat J (2001) The ABI1 and ABI2 protein phosphatases 2C act in a negative feedback regulatory loop of the abscisic acid signalling pathway. Plant J 25: 295-303.

Meyer K, Leube MP, Grill E (1994) A protein phosphatase 2C involved in ABA signal transduction in *Arabidopsis thaliana*. Science 264: 1452-1455.

Michaels SD, Amasino RM (1999) The gibberellic acid biosynthesis mutant ga1-3 of *Arabidopsis thaliana* is responsive to vernalization. Dev Genet 25: 194-198.

Monaghan J, Xu F, Gao M, Zhao Q, Palma K, Long C, Chen S, Zhang Y, Li X (2009)

Two Prp19-like U-box proteins in the MOS4-associated complex play redundant roles in plant innate immunity. PLoS Pathog 5: e1000526.

Monaghan J, Xu F, Xu S, Zhang Y, Li X (2010) Two putative RNA-binding proteins function with unequal genetic redundancy in the MOS4-associated complex. Plant Physiol 154: 1783-1793.

Montaville P, Dai Y, Cheung CY, Giller K, Becker S, Michalak M, Webb SE, Miller AL, Krebs J (2006) Nuclear translocation of the calcium-binding protein ALG-2 induced by the RNA-binding protein RBM22. Biochim Biophys Acta 1763: 1335-1343.

Mudgil Y, Uhrig JF, Zhou J, Temple B, Jiang K, Jones AM (2009) Arabidopsis N-MYC DOWNREGULATED-LIKE1, a positive regulator of auxin transport in a G protein-mediated pathway. Plant Cell 21: 3591-3609.

Murata Y, Pei ZM, Mori IC, Schroeder J (2001) Abscisic acid activation of plasma membrane Ca(2+) channels in guard cells requires cytosolic NAD(P)H and is differentially disrupted upstream and downstream of reactive oxygen species production in abi1-1 and abi2-1 protein phosphatase 2C mutants. Plant cell 13: 2513-2523.

Mustilli A, Merlot S, Vavasseur A, Fenzi F, Giraudat J (2002) Arabidopsis OST1 protein kinase mediates the regulation of stomatal aperture by abscisic acid and acts upstream of reactive oxygen species production. Plant Cell 14: 3089-3099.

Nagai T, Ibata K, Park ES, Kubota M, Mikoshiba K, Miyawaki A (2002) A variant of yellow fluorescent protein with fast and efficient maturation for cell-biological applications, Nat. Biotechnol. 20: 87-90.

Neuhaus G, Bowler C, Kern R, Chua NH (1993) Calcium/calmodulin-dependent and -independent phytochrome signal transduction pathways. Cell 73: 937-952.

Neumann FR, Nurse P (2007) Nuclear size control in fission yeast. J Cell Biol 179: 593-600.

Pan Q, Shai O, Lee LJ, Frey BJ, Blencowe BJ (2008) Blencowe, Deep surveying of alternative splicing complexity in the human transcriptome by high-throughput

sequencing. Nat Genet 40: 1413-1415.

Pandey S, Chen JG, Jones AM, Assmann SM (2006) G-protein complex mutants are hypersensitive to abscisic acid regulation of germination and postgermination development. Plant Physiol 141: 243-256.

Park JH, Scheerer P, Hofmann KP, Choe HW, Ernst OP (2008) Crystal structure of the ligand-free G-protein-coupled receptor opsin. Nature 454: 183-187.

Park SY, Fung P, Nishimura N, Jensen DR, Fujii H, Zhao Y, Lumba S, Santiago J, Rodrigues A, Chow TF, Alfred SE, Bonetta D, Finkelstein R, Provart NJ, Desveaux D, Rodriguez PL, McCourt P, Zhu JK, Schroeder JI, Volkman BF, Cutler SR (2009) Abscisic acid inhibits type 2C protein phosphatases via the PYR/PYL family of START proteins. Science 324: 1068-1071.

Pierce KL, Premont RT, Lefkowitz RJ (2002) Seven-transmembrane receptors. Nat Rev Mol Cell Biol 3: 639-650.

Pierre, M, Traverso, J. Boisson, B, Domenichini, S, Bouchez, D, Giglione, C, and Meinnel, T (2007) N-myristoylation regulates the SnRK1 pathway in Arabidopsis. Plant Cell 19: 2804-2821.

Pomeranz M, Finer J, Jang JC (2011) Putative molecular mechanisms underlying tandem CCCH zinc finger protein mediated plant growth, stress, and gene expression responses. Plant Signal Behav 6: 647-651.

Pomeranz MC, Hah C, Lin PC, Kang SG, Finer JJ, Blackshear PJ, Jang JC (2010) The Arabidopsis tandem zinc finger protein AtTZF1 traffics between the nucleus and cytoplasmic foci and binds both DNA and RNA. Plant Physiol 152: 151-165.

Puvion E, Viron A, Assens C, Leduc EH, Jeanteur P (1984) Immunocytochemical identification of nuclear structures containing snRNPs in isolated rat liver cells. J Ultrastruct Res 87: 180-189.

Quintero FJ, Ohta M, Shi H, Zhu JK, Pardo JM (2002) Reconstitution in yeast of the Arabidopsis SOS signaling pathway for Na^+ homeostasis. Proceedings of the National Academy of Sciences of the United States of America 99: 9061-9066.

Rappsilber J, Ryder U, Lamond AI, Mann M (2002) Large-scale proteomic analysis of

the human spliceosome. Genome Res 12: 1231-1245.

Resh MD (1999) Fatty acylation of proteins: new insights into membrane targeting of myristoylated and palmitoylated proteins, Biochim. Biophys. Acta 145: 11-16.

Reuter R, Appel B, Bringmann P, Rinke J, Lührmann R (1984) 5'-Terminal caps of snRNAs are reactive with antibodies specific for 2,2,7-trimethylguanosine in whole cells and nuclear matrices. Double-label immunofluorescent studies with anti-m3G antibodies and with anti-RNP and anti-Sm autoantibodies. Exp Cell Res 15: 548-560.

Rodriguez PL, Benning G, Grill E (1998) ABI2, a second protein phosphatase 2C involved in abscisic acid signal transduction in Arabidopsis. FEBS letters 421: 185-190.

Rosenbaum DM, Rasmussen SG, Kobilka BK (2009) The structure and function of G-protein-coupled receptors. Nature 459: 356-363.

Ru Y, Wang BB, Brendel V (2008) Spliceosomal proteins in plants. Curr Top Microbiol Immunol 326: 1-15.

Samach A, Onouchi H, Gold SE, Ditta GS, Schwarz-Sommer Z, Yanofsky MF, Coupland G (2000) Distinct roles of CONSTANS target genes in reproductive development of Arabidopsis. Science 288: 1613-1616.

Scheerer P, Park JH, Hildebrand PW, Kim YJ, Krauss N, Choe HW, Hofmann KP, Ernst OP (2008) Crystal structure of opsin in its G-protein-interacting conformation. Nature 455: 497-502

Schweighofer A, Hirt H, Meskiene I (2004) Plant PP2C phosphatases: emerging functions in stress signaling. Trends Plant 9: 236-243.

Searle I, He Y, Turck F, Vincent C, Fornara F, Kröber S, Amasino RA, Coupland G (2006) The transcription factor FLC confers a flowering response to vernalization by repressing meristem competence and systemic signaling in Arabidopsis. Genes Dev 20: 898-912.

Seki M, Narusaka M, Kamiya A, Ishida J, Satou M, Sakurai T, Nakajima M, Enju A, Akiyama K, Oono Y, Muramatsu M, Hayashizaki Y, Kawai J, Carninci P, Itoh M,

Ishii Y, Arakawa T, Shibata K, Shinagawa A, Shinozaki K (2002) Functional annotation of a full-length Arabidopsis cDNA collection. Science 296: 141-145.

Sheen J (1998) Mutational analysis of protein phosphatase 2C involved in abscisic acid signal transduction in higher plants. Proc Natl Acad Sci U S A 95: 975-980.

Sheldon CC, Burn JE, Perez PP, Metzger J, Edwards JA, Peacock WJ, Dennis ES (1999) The FLF MADS box gene: a repressor of flowering in Arabidopsis regulated by vernalization and methylation. Plant cell 11: 445-458.

Sheldon CC, Hills MJ, Lister C, Dean C, Dennis ES, Peacock WJ (2008) Resetting of FLOWERING LOCUS C expression after epigenetic repression by vernalization. Proc Natl Acad Sci 105: 2214-2219.

Shen W, Reyes, MI, Hanley-Bowdoin L (2009) Arabidopsis protein kinases GRIK1 and GRIK2 specifically activate SnRK1 by phosphorylating its activation loop. Plant physiol 150: 996-1005.

Simonds WF, Woodard GE, Zhang JH (2004) Assays of nuclear localization of R7/Gbeta5 complexes. Methods Enzymol 390: 210-223.

Smaczniak C, Immink RG, Angenent GC, Kaufmann K (2012) Developmental and evolutionary diversity of plant MADS-domain factors: insights from recent studies. Development 139: 3081-3098.

Soderman E, Mattsson J, Engstrom P (1996) The Arabidopsis homeobox gene ATHB-7 is induced by water deficit and by abscisic acid. Plant J 10: 375-381.

Spector DL and Lamond AI (2012) Nuclear speckles. Cold Spring Harb Perspect Biol. 3: pii:a000646.

Spector DL, Schrier WH, Busch H (1983) Immunoelectron microscopic localization of snRNPs. Biol. Cell 49: 1-10.

Stewart M (2000) Insights into the molecular mechanism of nuclear trafficking using nuclear transport factor 2 (NTF2). Cell Struct Funct 25: 217-255.

Stolc V, Gauhar Z, Mason C, Halasz G, van Batenburg MF, Rifkin SA, Hua S, Herreman T, Tongprasit W, Barbano PE, Bussemaker HJ, White KP (2004) A gene expression map for the euchromatic genome of Drosophila melanogaster.

Science 306: 655-660.

Strizhov N, Abraham E, Okresz L, Blickling S, Zilberstein A, Schell J, Koncz C, Szabados L (1997) Differential expression of two P5CS genes controlling proline accumulation during salt-stress requires ABA and is regulated by ABA1, ABI1 and AXR2 in Arabidopsis. Plant J 12: 557-569.

Sugden C, Crawford RM, Halford NG, and Hardie DG (1999) Regulation of spinach SNF1-related (SnRK1) kinases by protein kinases and phosphatases is associated with phosphorylation of the T loop and is regulated by 5'-AMP. Plant J 19: 433-439.

Sun J, Jiang H, Xu Y, Li H, Wu X, Xie Q, Li C (2007) The CCCH-type zinc finger proteins AtSZF1 and AtSZF2 regulate salt stress responses in Arabidopsis. Plant Cell Physiol 48: 1148-1158.

Takeda S, Matsumoto N, Okada K (2004) RABBIT EARS, encoding a SUPERMAN-like zinc finger protein, regulates petal development in *Arabidopsis thaliana*. Development 131: 425-434.

Tarn WY, Hsu CH, Huang KT, Chen HR, Kao HY, Lee KR, Cheng SC (1994) Functional association of essential splicing factor(s) with PRP19 in a protein complex. EMBO J 13: 2421-2431.

Telfer A, Bollman KM, Poethig RS (1997) Phase change and the regulation of trichome distribution in *Arabidopsis thaliana*. Development 124: 645-654.

Torrecilla I, Spragg EJ, Poulin B, McWilliams PJ, Mistry SC, Blaukat A, Tobin AB (2007) Phosphorylation and regulation of a G protein-coupled receptor by protein kinase CK2, J. Cell Biol. 177: 127-137.

Trusov Y, Rookes JE, Tilbrook K, Chakravorty D, Mason MG, Anderson DJ, Chen JG, Jones AM, Botella JR (2007) Heterotrimeric G protein γ subunits provide functional selectivity in Gβγ dimer signaling in Arabidopsis, Plant Cell 19: 1235-1250.

Trusov Y, Sewelam N, Rookes JE, Kunkel M, Nowak E, Schenk PM, Botella JR (2009) Heterotrimeric G proteins-mediated resistance to necrotrophic pathogens

includes mechanisms independent of salicylic acid-, jasmonic acid/ethylene- and abscisic acid-mediated defense signaling. Plant J 58: 69-81.

Tsugama D, Liu S, Takano T (2012) A putative myristoylated 2C-type protein phosphatase, PP2C74, interacts with SnRK1 in Arabidopsis. FEBS Lett 5866: 693-698.

Ueguchi-Tanaka M, Fujisawa Y, Kobayashi M, Ashikari M, Iwasaki Y, Kitano H, Matsuoka M (2000) Rice dwarf mutant d1, which is defective in the alpha subunit of the heterotrimeric G protein, affects gibberellin signal transduction. Proc Natl Acad Sci U S A 97: 11638-11643.

Ullah H, Chen JG, Temple B, Boyes DC, Alonso JM, Davis KR, Ecker JR, Jones AM (2003) The beta-subunit of the Arabidopsis G protein negatively regulates auxin-induced cell division and affects multiple developmental processes. Plant Cell 15: 393-409.

Ullah H, Chen JG, Wang S, Jones AM (2002) Role of a heterotrimeric G protein in regulation of Arabidopsis seed germination. Plant Physiol 29: 897-907.

Ullah H, Chen JG, Young JC, Im KH, Sussman MR, Jones AM (2001) Modulation of cell proliferation by heterotrimeric G protein in Arabidopsis. Science 292: 2066-2069

Umbrasaite J, Schweighofer A, Kazanaviciute V, Magyar Z, Ayatollahi Z, Unterwurzacher V, Choopayak C, Boniecka J, Murray JA, Bogre L, Meskiene I (2010) MAPK Phosphatase AP2C3 Induces Ectopic Proliferation of Epidermal Cells Leading to Stomata Development in Arabidopsis. PLoS One 5: e15357.

Umezawa T, Sugiyama N, Mizoguchi M, Hayashi S, Myouga F, Yamaguchi-Shinozaki K, Ishihama Y, Hirayama T, Shinozaki K (2009) Type 2C protein phosphatases directly regulate abscisic acid-activated protein kinases in Arabidopsis. Proc Natl Acad Sci U S A 106: 17588-17593.

Valadkhan S, Jaladat Y (2010) The spliceosomal proteome: at the heart of the largest cellular ribonucleoprotein machine. Proteomics 10: 4128-4141

Venter JC, *et al*. (2001) The sequence of the human genome. Science 291: 1304-1351.

Wahl MC, Will CL, Lührmann R (2009) The spliceosome: design principles of a dynamic RNP machine. Cell 136: 701-718.

Wang S, Narendra S, Fedoroff N (2007) Heterotrimeric G protein signaling in the Arabidopsis unfolded protein response, Proc. Natl. Acad. Sci. U. S. A. 104: 3817-3822.

Wang XQ, Ullah H, Jones AM, Assmann SM (2001) G protein regulation of ion channels and abscisic acid signaling in Arabidopsis guard cells. Science 292: 2070-2072.

Warpeha KM, Hamm HE, Rasenick MM, Kaufman LS (1991) A blue-light-activated GTP-binding protein in the plasma membranes of etiolated peas. Proc Natl Acad Sci U S A 88: 8925-8929.

Wei Q, Zhou W, Hu G, Wei J, Yang H, Huang J (2008) Heterotrimeric G-protein is involved in phytochrome A-mediated cell death of Arabidopsis hypocotyls, Cell Res. 18: 949-960.

Weiss C, Garnaat C, Mukai K, Hu Y, Ma H (1994) Isolation of cDNAs encoding guanine nucleotide-binding protein β-subunit homologues from maize (ZGB1) and Arabidopsis (AGB1). Proc Natl Acad Sci U S A 91: 9554-9558.

Willard FS, Crouch MF (2000) Nuclear and cytoskeletal translocation and localization of heterotrimeric G-proteins. Immunol Cell Biol. 78: 387-394.

Wu FH, Shen SC, Lee LY, Lee SH, Chan MT, Lin CS (2009) Tape-Arabidopsis Sandwich - a simpler Arabidopsis protoplast isolation method. Plant Methods 24: 5-16.

Xiong L, Ishitani M, Zhu JK (1999) Interaction of osmotic stress, temperature, and abscisic acid in the regulation of gene expression in Arabidopsis. Plant Physiol 119: 205-212.

Xu D, Friesen JD (2001) Splicing factor slt11p and its involvement in formation of U2/U6 helix II in activation of the yeast spliceosome. Mol Cell Biol 21: 1011-1023.

Xue T, Wang D, Zhang S, Ehlting J, Ni F, Jakab S, Zheng C, Zhong Y (2008)

Genome-wide and expression analysis of protein phosphatase 2C in rice and Arabidopsis BMC Genomics. 9: 550.

Yoshida R, Hobo T, Ichimura K, Mizoguchi T, Takahashi F, Aronso J, Ecker JR, Shinozaki K (2002) ABA-activated SnRK2 protein kinase is required for dehydration stress signaling in Arabidopsis. Plant Cell Physiol 43: 1473-1483.

Acknowledgement

Firstly, I would like to express my deepest appreciation to my supervisor, Dr. Takano Tetsuo, for his creative guidance and continuous discussion throughout my doctor course.

Secondly, I would like to express my heartfelt gratitude to Dr. Liu Shenkui of Northeast Forestry University, for his precious suggestions and comments of my research.

Thirdly, I must owe my sincere gratitude to my fellows and my friends, Dr. Daisuke Tsugama, Dr. Feifei Qin, Dr. Jeeraporn Kansup, Dr. Xuejia Li, Dr. Qian Sun, Dr. Shio Kobayashi, Master Michi Oya, Master Fumiya Sugiyama and Madam Yamamoto.

Lastly, my thanks would go to my beloved family for their loving considerations and great confidence. I believe the doctor course will be in my good memory until eternity.

This study was partially supported by a grant from the China Scholarship Council (CSC).

Hua LIU

PhD Candidate

Graduate School of Agricultural and Life Sciences

The University of Tokyo

Dated 14 December 2012